University of Minnesota Duluth
Department of Mathematics and Statistics

Modeling of Ebola Control Strategies

Duluth, May 2016

Václav Hasenöhrl

Acknowledgments

I would like to express my appreciation to Dr. Harlan Stech and Dr. Bruce Peckham for their support and patience as my advisors. Their critiques and advice were valuable assets while working on this paper. My thanks should also be extended to the faculty and staff of the department of Mathematics and Statistics at University of Minnesota Duluth. Together they provided a daily support and guidance that made for a great learning environment. I would also like to thank Dr. Yang Li for serving on my committee. I would like to give special thanks to my family and closest friends who made all of this possible and helped me as I studied abroad. I am also grateful for their constant support and encouragement.

Abstract

In the last two years Ebola has filled news headlines more than ever, it is mainly because of the large outbreak in West Africa in 2014-2015 with thousands of casualties. What are the options for control of this deadly disease? This paper provides an innovative model of Ebola transmission and discusses three control strategies: hospitalization, burial teams, and probability of seeking hospitalization. By varying certain parameters we measure the effectiveness of these interventions and we focus on suggesting solutions.

Keywords: Basic Epidemic Models, Advanced Epidemic Models, Ebola Models, Ebola Control Strategies, Hospitalization, Burial Teams, Probability of Seeking Hospitalization

Contents

1 Introduction

Origins of mathematical modeling of infectious diseases go back to the early 1900's. With an increasing risk of population illnesses in the society, disease modeling has become a significant part of epidemic control. Mathematical models can project how infectious illnesses progress, predict an epidemic, or help us to calculate the effects of possible interventions. Over time many models have been developed and it is not a surprise that different diseases require specific ways of modeling them. Possible questions as the following can arise. Does there exist a cure for the disease? Can people catch the disease multiple times? Is there a known vaccine for the disease? One has to consider all these options to create a meaningful model. As the topic of this paper suggests, the focus of our work was on one specific disease, Ebola.

"Ebola, previously known as Ebola hemorrhagic fever, is a rare and deadly disease caused by infection with one of the Ebola virus species. Ebola can cause disease in humans and nonhuman primates (monkeys, gorillas, and chimpanzees). Ebola is caused by an infection with a virus of the family Filoviridae, genus Ebolavirus. There are five identified Ebola virus species, four of which are known to cause disease in humans. Ebola viruses are found in several African countries. Ebola was first discovered in 1976 near the Ebola River in what is now the Democratic Republic of the Congo. Since then, outbreaks have appeared sporadically in Africa, up until the last decade. People get Ebola through direct contact (through broken skin or mucous membranes in, for example, the eyes, nose, or mouth) with blood or body fluids of a person who is sick with or has died from Ebola, objects (like needles and syringes) that have been contaminated with body fluids from a person who is sick with Ebola or the body of a person who has died from Ebola." [1].

The interest in modeling Ebola has recently increased as a consequence of outbreaks in West Africa. The outbreak in 2014-2015 was the largest one in history of this disease, with multiple countries affected. The outbreak began in Guinea on March 23, 2014 [13], and spread to yield widespread and intense transmission in Guinea, Liberia, and Sierra Leone, as well as cases in five additional countries (Nigeria, Senegal, Mali, Spain, USA) [5], with over 28,000 cases by March 2016. [7]. Having a good model would allow people to make reliable predictions of the possible future spread of the disease and stop it before an outbreak. One of the key factors of the spread of Ebola was also a lack of information among people in these countries. For example, people there still perform traditional burials where the possibility of catching Ebola is extremely high. This with other aspects made the fight against Ebola even harder.

Ebola is usually modeled with a system of deterministic differential equations, based on the very first models by W. O. Kermack and A .G. McKendrick in 1927 [3]. The derivation of this and other simple models is provided in the next chapter.

2 Derivation of the Simplest Epidemic Models

2.1 SI Model

This chapter will introduce approaches of creating a mathematical disease model. We assume that we are modeling a disease in a population of constant size, N. This means there are no new people born, or individuals leaving the population (for example migration). We define a compartment $I(t)$ as the number of people infectious at time t. Note that infectious means that an individual has the disease and can spread it to someone else. As a second compartment we shall define $S(t)$ to be the number of people susceptible to the disease at time t. By assumption $I(t) + S(t) = N$. An important task is to define a rate at which contacts among the population are made and where there is a chance for the illness to spread. We will call this rate simply the *contact rate* and denote it by β.

Remark 2.1. Note that one might assume that the contact rate β is proportional to the size of a population N, which yields the number of contacts of an individual with others to be βN. For example, this approach is used in [4]. As those authors say themselves, this is rather unrealistic, because not everyone can make a contact with everyone else based on a structure of a country, etc.

We assume that the population is homogeneous, and we define β to be the number of effective (this means a contact, if between an infective and a susceptible, would be sufficient to transmit infection) contacts per any individual per unit time. Based on this, since the probability that a random contact by an infectious person is with a susceptible is $\frac{S(t)}{N}$, then the number of new infections per unit time and per each infectious person is $\beta\frac{S(t)}{N}$. This gives a rate of new infections $\beta\frac{S(t)}{N}I(t)$. Thus, the rate of change $\dot{I}(t)$ (the *dot* denotes the derivative in respect to time t) of the number of infectious individuals is given by the following differential equation:

$$\begin{aligned}\dot{I}(t) &= \beta\frac{S(t)}{N}I(t),\\ \dot{I}(t) &= \beta\left(1-\frac{I}{N}\right)I, \quad \text{since } S = N - I.\end{aligned}$$

The full model with an initial condition is then:

$$\begin{cases}\dot{I}(t) &= \beta\left(1-\frac{I}{N}\right)I,\\ I(0) &= I_0.\end{cases} \tag{M2.1}$$

Since compartment I is assumed to be non-negative and $I \leq N$, then $1 - \frac{I}{N} \geq 0$. Also, $\beta > 0$, therefore $\dot{I}(t) \geq 0$. This means that $I(t)$ is a non-decreasing function bounded by N from above. Hence, it has a limit for any $I_0 > 0$. The simplicity of this model even allows us to solve it explicitly, so we could show that the limit is actually N. The sense of qualitative behavior can be seen in Figure 1.

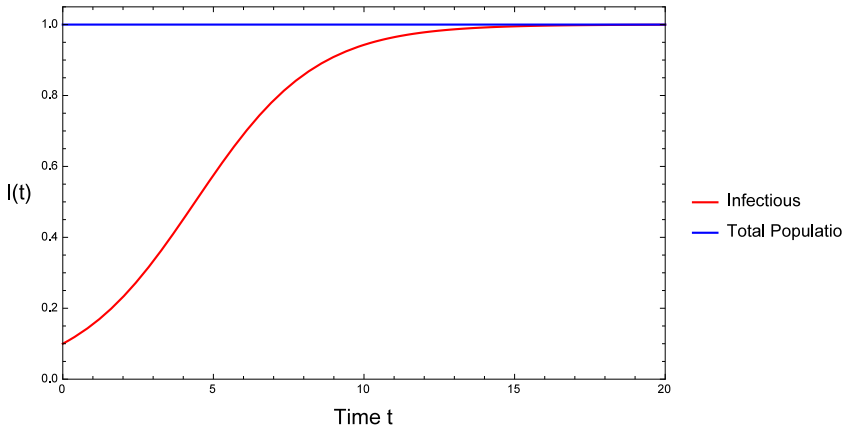

Figure 1: Solution to the system (M2.1) *with* $I_0 = 0.1, N = 1, \beta = 0.5$.

This model represents a situation when the whole population becomes eventually infected. Once an individual gets the disease, it is not lethal, neither can it be cured. Thanks to this very simple model, one can get an impression how disease modeling works in general. However, such a simplistic model would not likely be applicable to any real disease, especially Ebola.

Remark 2.2. For the sake of brevity we might write S instead of $S(t)$ since the time dependence is rather obvious. This applies to other compartments as well. We will use this shorter notation for all the following models.

2.2 SIR Model

As a next step in the introduction to epidemic modeling, we will mention the model introduced by W. O. Kermack and A. G. McKendrick in 1927 [3]. It is considered to be one of the very first epidemiology models and it is used as a stepping stone for future work. Their model is formed by three stages. In other words, population is divided into three different groups. As in the previous model, we consider the two compartment groups of susceptible $S(t)$ and infectious $I(t)$. In addition to these two, a third

class $R(t)$ of people who recover from the disease is introduced. A standard assumption in epidemic models is that the rate of recovery is proportionate to the number of infected individuals. Let us denote the proportionality constant by $\alpha > 0$, then the rate of recovery is $\alpha I(t)$. All together we get the following system of differential equations:

$$\begin{aligned} \frac{\mathrm{d}S}{\mathrm{d}t} &= -\frac{1}{N}\beta SI, \\ \frac{\mathrm{d}I}{\mathrm{d}t} &= \frac{1}{N}\beta SI - \alpha I, \\ \frac{\mathrm{d}R}{\mathrm{d}t} &= \alpha I. \end{aligned} \tag{M2.2}$$

Remark 2.3. The assumption that the recovery rate is proportionate to the number of infected individuals comes from the fact that the constant α determines the average length of an individual being infected as $\frac{1}{\alpha}$. This can be shown by solving the second equation of the SIR model, while considering no new infections to the system. ($\frac{\mathrm{d}I}{\mathrm{d}t} = 0 - \alpha I, I(0) = I_0 \Rightarrow I(t) = I_0 e^{-\alpha t}$. This is the exponential distribution with mean $\frac{1}{\alpha}$.)

The flow chart of the SIR model is shown below. We can see that people who recover do not return to the group of susceptible. How does this modification affect the spread of a disease compared to the SI model? We will answer this question by the following analysis of (M2.2).

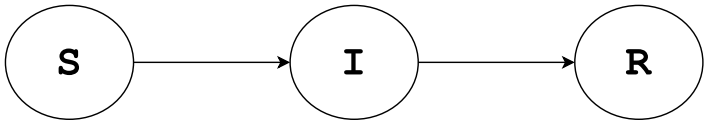

Figure 2: Flow chart of the SIR model (M2.2).

Although this model has still only three equations, our options for solving it explicitly are already limited due to the non-linearity of the first two equations. More about finding a solution can be found in [3], but it is not a standard solution in sense that we cannot find an explicit formula for S, I, and R respectively. Fortunately, there is another more general approach which can be used to analyze this and other more complicated systems.

Note that $S' + I' + R' = 0$. This corresponds to our assumption that the population remains constant. This fact is one of the immediate flaws of this model. What about people who die from the sickness and are no longer infected? What about newborn people? What about people who die without being sick? On the other hand, we

can argue that in short-term, newborn and dead people do not significantly affect the size of the population, so we can still use this approach as a reasonable approximation. Consider an initial population of susceptible S_0 and let us introduce an initial group of infectious I_0, then $N = S_0 + I_0$. It is important to observe that all the compartments in the model are assumed to be non-negative differentiable functions. The starting point of our analysis is to add the first two equations of (M2.2).

$$S' + I' = -\alpha I. \tag{2.1}$$

This means that $(S + I)' < 0$. Therefore, the function $S + I$ is a non-negative differentiable non-increasing function bounded by 0. Therefore, $S + I$ has a constant limit which implies that $\lim_{t\to\infty}(S + I)' = 0$. Hence, from (2.1) we get $\lim_{t\to\infty} I = I_\infty = 0$.

Now, by integrating (2.1) from 0 to ∞, we get

$$\int_0^\infty S' d\tau + \int_0^\infty I' d\tau = -\alpha \int_0^\infty I d\tau,$$

$$S_0 - S_\infty + I_0 - I_\infty = \alpha \int_0^\infty I d\tau.$$

Next, divide the first equation of (M2.2) by S and integrate it from 0 to ∞ to get the following

$$\begin{aligned}
\log \frac{S_0}{S_\infty} &= \frac{1}{N}\beta \int_0^\infty I d\tau, \\
&= \frac{1}{N}\frac{\beta}{\alpha}\left[S_0 - S_\infty + I_0 - I_\infty\right], \\
&= \frac{1}{N}\frac{\beta}{\alpha}\left[S_0 - S_\infty + I_0\right], \\
&= \frac{1}{N}\frac{\beta}{\alpha}\left[N - S_\infty\right], \\
&= \frac{\beta}{\alpha}\left[1 - \frac{S_\infty}{N}\right].
\end{aligned} \tag{2.2}$$

The expression (2.2) is called the *final size relation*. The fraction $\frac{\beta}{\alpha}$ is called the *basic reproduction number* and is denoted by $\mathcal{R}_0$.

Definition 1. The (basic) reproduction number $\mathcal{R}_0$ is the number of secondary infections caused by a single infectious individual introduced into a wholly susceptible population of size N.

If $\mathcal{R}_0 < 1$, then an infected individual produces on average less than one new infection over the course of its infectious period, and the infection cannot grow. On the contrary, if $\mathcal{R}_0 > 1$, then each infected individual produces, on average, more than one new infection, and the disease can spread into the population [9]. This is why $\mathcal{R}_0$ is sometimes called the *threshold parameter*.

More detailed descriptions of the final size relation and the reproduction number with formal definitions can be found in [9], or in [10]. It is important to say that the basic reproduction number is related to the disease-free equilibrium. We will show the methods described in [9] and in [10] later on a specific example.

The simplicity of the SIR model also allows us to demonstrate directly the meaning of $\mathcal{R}_0$. Consider the second equation

$$\begin{aligned}\frac{\mathrm{d}I}{\mathrm{d}t} &= \frac{1}{N}\beta SI - \alpha I,\\ &= I\left[\frac{S}{N}\beta - \alpha\right].\end{aligned}$$

See that, if

$$\frac{S_0}{N}\beta - \alpha < 0, \tag{2.3}$$

then I is a decreasing function for all t. This means that the number of infectious people will be decreasing from the beginning of an outbreak (no epidemic). Conversely, if

$$\frac{S_0}{N}\beta - \alpha > 0, \tag{2.4}$$

then I is an increasing function as long as $\frac{S}{N} > \frac{\alpha}{\beta}$. Thus, the number of infectious individuals will be increasing initially (epidemic), but since S is decreasing for all t, then I reaches its maximum at $\frac{S}{N} = \frac{\alpha}{\beta}$, and then decreases to 0 as shown above. Considering the definition of $\mathcal{R}_0$, we assume that the system is in a disease-free equilibrium. Hence, $S_0 = N$ (or $S_0 \approx N$, meaning that the initial number of infectious people is very small compared to the magnitude of N). This can be understood as having a population of susceptibles into which we introduce an outside infectious individual. Therefore, inequalities (2.3) and (2.4) become

$$\frac{\beta}{\alpha} < 1, \quad \frac{\beta}{\alpha} > 1 \text{ respectively.}$$

We can see that this matches the term found above for the basic reproduction number for the SIR model (M2.2). Note that we are able to directly explain the meaning of $\mathcal{R}_0$ only because the SIR model is simple. The qualitative behavior of the two possibilities (epidemic or no epidemic) is shown below.

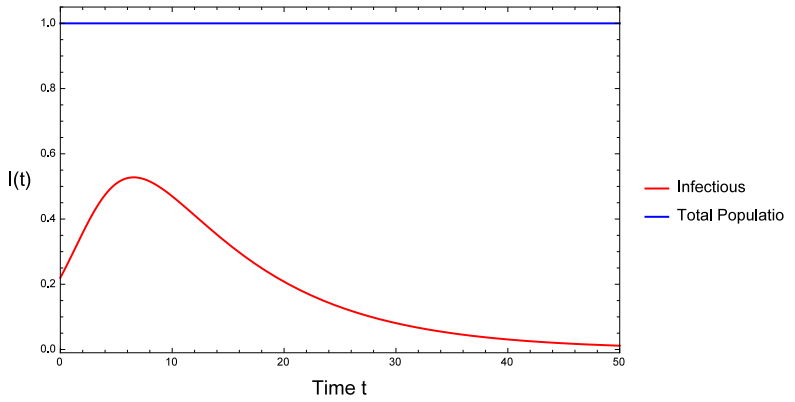

Figure 3: Solution to the system (M2.2) *with* $I_0 = 0.1, N = 1, \frac{\beta}{\alpha} = 5$.

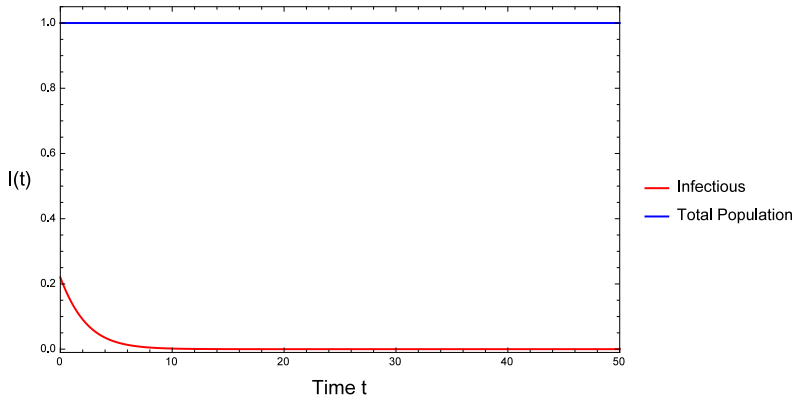

Figure 4: Solution to the system (M2.2) *with* $I_0 = 0.1, N = 1, \frac{\beta}{\alpha} = \frac{5}{8}$.

The pulse depicted in Figure 3 is typical for epidemic models. Moreover, the two behaviors, shown in Figures 3 and 4, are the only two outcomes we can obtain for the models we are dealing with. This is because individuals do not cycle between the compartments. We explain this by the fact the for Ebola, if one survives the disease, a long lasting immunity is granted.

This chapter presented the basic SIR model and ways to analyze it. We showed that if the recovered compartment is introduced, meaning that individuals can recover from the disease, the function $I(t)$ limits to zero, whereas the function S approaches a positive limit as $t \to \infty$. This limit can be computed using the final size relation. Another application of the final size relation is to actually estimate the parameters of our model. One could track an ongoing outbreak of a certain disease and then retrospectively use the relation (2.2), by knowing how many people got the disease, to determine the contact rate β. This is actually the crucial part of creating a meaningful model. However, it is not an easy question, because the contact rate β depends on many factors. For example, population size and density, effectiveness of hospital care, safe burials of diseased people, etc.

Clearly, the SIR model is not perfect. However, it is a good starting epidemic model and since it is rather simple, we can use it to develop analytical tools suitable for the analysis. Which, as we will show later, are applicable to more complicated models as well.

2.3 SEIR Model

An immediate extension to the SIR model is a SEIR model. This model adds an "exposed" compartment to the system. For many diseases there is usually an exposed (incubation) period after the transmission of the disease, during which the individual is infected but not infectious yet (or does not show any symptoms to be able to spread the disease). This is typical for diseases such as HIV, Mononucleosis, Chickenpox, Mumps, etc. For Ebola, the incubation period ranges from 2 - 21 days [12].

The model becomes

$$\begin{aligned} \frac{\mathrm{d}S}{\mathrm{d}t} &= -\frac{1}{N}\beta SI, \\ \frac{\mathrm{d}E}{\mathrm{d}t} &= \frac{1}{N}\beta SI - \kappa E, \\ \frac{\mathrm{d}I}{\mathrm{d}t} &= \kappa E - \alpha I, \\ \frac{\mathrm{d}R}{\mathrm{d}t} &= \alpha I. \end{aligned} \tag{M2.3}$$

with the following flow chart:

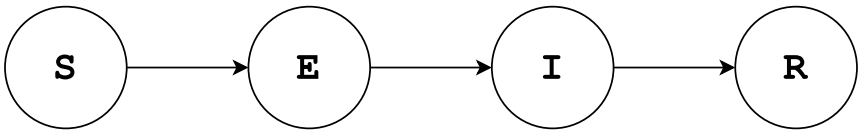

Figure 5: Flow chart of SEIR model (M2.3).

We introduce a new constant κ, which gives us the average length, $\frac{1}{\kappa}$, of the incubation period. This model is more realistic than the SIR model but for the purposes of this work, it is still rather simple.

Other examples of models such as Treatment Model, A Quarantine-Isolation Model, Models with Disease Deaths, A Vaccination Model can be found in [4].

3 Ebola Related Models

3.1 Example 1 - Legrand Model of Hospitalization

The intention of this chapter is to provide examples of actual models used for transmission of Ebola. The first one is a model from a paper from 2007 by J. Legrand, et al. [11]. This model is an extension to the SEIR model shown in the previous chapter. It still contains susceptible, exposed, infectious, and removed classes, but the authors also introduce hospital and funeral classes. The hospital compartment simply represents people who occupy a bed in a hospital. The funeral class represents people who died but have not been buried yet. Thus, they can still spread the disease. The system of differential equations is the following:

$$\begin{aligned}
\frac{\mathrm{d}S}{\mathrm{d}t} &= -\frac{1}{N}\left[b_I SI + b_H SH + b_F SF\right], \\
\frac{\mathrm{d}E}{\mathrm{d}t} &= \frac{1}{N}\left[b_I SI + b_H SH + b_F SF\right] - aE, \\
\frac{\mathrm{d}I}{\mathrm{d}t} &= aE - \left[c_h h_1 + c_i(1-h_1)(1-d_1) + c_d(1-h_1)d_1\right] I, \\
\frac{\mathrm{d}H}{\mathrm{d}t} &= c_h h_1 I - \left[c_{dh} d_2 + c_{ih}(1-d_2)\right] H, \\
\frac{\mathrm{d}F}{\mathrm{d}t} &= c_d(1-h_1)d_1 I + c_{dh} d_2 H - c_f F, \\
\frac{\mathrm{d}R}{\mathrm{d}t} &= c_i(1-h_1)(1-d_1) I + c_{ih}(1-d_2) H + c_f F.
\end{aligned} \tag{M3.1}$$

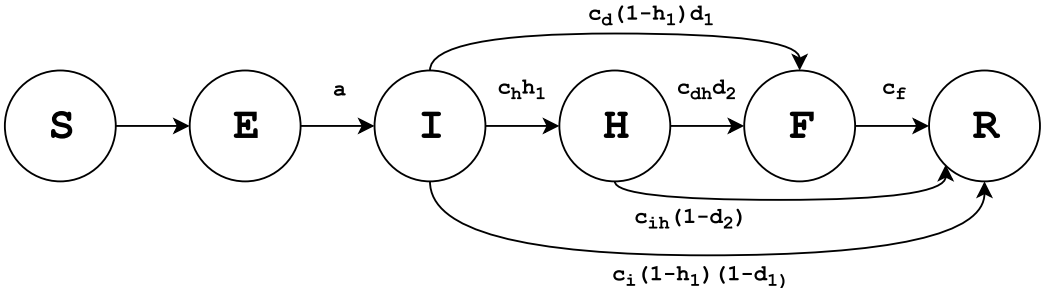

Figure 6: Flow chart of Legrand model (M3.1)

We will not describe the model (M3.1) any further. More information on the parameters and results for this model can be found in the paper [11]. Our goal at this point is

to demonstrate the computation for finding the reproduction number $\mathcal{R}_I$ and the final size relation. Similar analysis, as shown for the SIR model, can be also done for this model.

3.1.1 Reproduction Number $\mathcal{R}_0$ - Basic Integration Method

This section will describe the extended method from [10] for obtaining the reproduction number $\mathcal{R}_0$ and the limited size relation. We will demonstrate the method on the Legrand model mentioned above.

The initial step is to divide the first equation of (M3.1) by S:

$$\frac{S'}{S} = -\frac{1}{N}\left[b_I I + b_H H + b_F F\right],$$

Integrate this equation from 0 to ∞:

$$\log\frac{S_0}{S_\infty} = \frac{1}{N}\left[b_I \int_0^\infty I dt + b_H \int_0^\infty H dt + b_F \int_0^\infty F dt\right]. \tag{3.1}$$

Add the first two equations of the system (M3.1) and integrate them from 0 to ∞:

$$\begin{aligned} S' + E' &= -aE, \\ a\int_0^\infty E dt &= -S_\infty + S_0 - E_\infty + E_0. \end{aligned}$$

Next, integrate third, fourth, and fifth equation of (M3.1) from 0 to ∞

$$\begin{aligned} \int_0^\infty I dt &= \frac{-I_\infty + I_0 + a\int_0^\infty E dt}{c_h h_1 + c_i(1-h_1)(1-d_1) + c_d(1-h_1)d_1}, \\ \int_0^\infty H dt &= \frac{-H_\infty + H_0 + c_h h_1 \int_0^\infty I dt}{c_{dh} d_2 + c_{ih}(1-d_2)}, \\ \int_0^\infty F dt &= \frac{-F_\infty + F_0 + c_d(1-h_1)d_1 \int_0^\infty I dt + c_{dh} d_2 \int_0^\infty H dt}{c_f}. \end{aligned}$$

Substitute in for the integrals on the right side of each equation.

$$\int_0^\infty I dt = \frac{-I_\infty + I_0 - S_\infty + S_0 - E_\infty + E_0}{c_h h_1 + c_i(1-h_1)(1-d_1) + c_d(1-h_1)d_1}, \tag{3.2}$$

$$\int_0^\infty H dt = \frac{-H_\infty + H_0 + c_h h_1 \frac{-I_\infty + I_0 - S_\infty + S_0 - E_\infty + E_0}{c_h h_1 + c_i(1-h_1)(1-d_1) + c_d(1-h_1)d_1}}{c_{dh} d_2 + c_{ih}(1-d_2)}, \tag{3.3}$$

$$\int_0^\infty F dt = \frac{-F_\infty + F_0 + c_d(1-h_1)d_1 \frac{-I_\infty + I_0 - S_\infty + S_0 - E_\infty + E_0}{c_h h_1 + c_i(1-h_1)(1-d_1) + c_d(1-h_1)d_1}}{c_f} + \tag{3.4}$$

$$+ \frac{c_{dh} d_2 \frac{-H_\infty + H_0 + c_h h_1 \frac{-I_\infty + I_0 - S_\infty + S_0 - E_\infty + E_0}{c_h h_1 + c_i(1-h_1)(1-d_1) + c_d(1-h_1)d_1}}{c_{dh} d_2 + c_{ih}(1-d_2)}}{c_f}.$$

Note that one of the assumptions for this model is $S + E + I + H + F + R = N$. Thus, the population remains constant. Also, we assume that the initial conditions are: $S(0) = S_0, E(0) = 0, I(0) = 0, H(0) = 0, F(0) = 0$. Therefore $S_0 = N$ which means that the population is initially in disease free equilibrium.

Recall that we were able to show that $I_\infty = 0$ for the SIR model. For the model (M3.1), by applying the similar procedure, we can show that $E_\infty = 0, I_\infty = 0, H_\infty = 0, F_\infty = 0$. The approach is as follows.

Remark 3.1. Note that all the compartmental functions S, E, I, H, F, R are assumed to be non-negative differentiable functions.

The first equality $E_\infty = 0$ can be obtained by adding equations for I, H, F, R. Then, we get:

$$I' + H' + F' + R' = aE,$$

which means that $I + H + F + R$ is a non-negative smooth non-decreasing function bounded by N. This implies that it has a limit as $t \to \infty$ (By Monotone Convergence Theorem). Therefore, the derivative of such function will limit to zero as $t \to \infty$. Hence, $E_\infty = 0$.

We proceed by adding equations for H, F, R and we get:

$$H' + F' + R' = \left[c_h h_1 + c_d(1-h_1)d_1 + c_i(1-h_1)(1-d_1)\right] I.$$

This shows that $H + F + R$ is a non-negative smooth non-decreasing function bounded by N. Hence, it has a limit as $t \to \infty$ and, similarly as in the previous case, its derivative

will limit to zero. Therefore, $I_\infty = 0$.

By adding equations for F, R we get:

$$F' + R' = [c_d(1-h_1)d_1 + c_i(1-h_1)(1-d_1)]\, I + [c_{dh}d_2 + c_{ih}(1-d_2)]\, H.$$

Again, this means that $F + R$ is a non-negative smooth non-decreasing function bounded by N. Thus, it has a limit as $t \to \infty$. It follows that derivative will limit to zero. We already know that $I_\infty = 0$, hence $H_\infty = 0$.

Finally, from the last equation, we get that R is a non-negative smooth non-decreasing function bounded by N. Therefore, it has a limit as $t \to \infty$, and in analogy to the previous case, its derivative will limit to zero as well. We already know that $I_\infty = 0, H_\infty = 0$. Hence, $F_\infty = 0$.

As the last step, we substitute the equations (3.2), (3.3), (3.4) for the integrals in (3.1) and we get:

$$\begin{aligned}
\log \frac{S_0}{S_\infty} = \frac{1}{N} \Bigg[& b_I \left(\frac{N - S_\infty}{c_h h_1 + c_i(1-h_1)(1-d_1) + c_d(1-h_1)d_1} \right) + \\
& + b_H \left(\frac{(N-S_\infty)c_h h_1}{c_{dh}d_2 + c_{ih}(1-d_2)} \frac{1}{c_h h_1 + c_i(1-h_1)(1-d_1) + c_d(1-h_1)d_1} \right) + \\
& + b_F \Bigg(\frac{(N-S_\infty)c_d(1-h_1)d_1}{c_h h_1 + c_i(1-h_1)(1-d_1) + c_d(1-h_1)d_1} \frac{1}{c_f} + \\
& \quad + \frac{\frac{(N-S_\infty)c_h h_1 c_{dh} d_2}{c_{dh}d_2 + c_{ih}(1-d_2)}}{c_h h_1 + c_i(1-h_1)(1-d_1) + c_d(1-h_1)d_1} \frac{1}{c_f} \Bigg) \Bigg]
\end{aligned}$$

Factor out $(N - S_\infty)$

$$\begin{aligned}
\log \frac{S_0}{S_\infty} = \left[1 - \frac{S_\infty}{N} \right] \Bigg[& b_I \left(\frac{1}{c_h h_1 + c_i(1-h_1)(1-d_1) + c_d(1-h_1)d_1} \right) + \\
& + b_H \left(\frac{c_h h_1}{c_{dh}d_2 + c_{ih}(1-d_2)} \frac{1}{c_h h_1 + c_i(1-h_1)(1-d_1) + c_d(1-h_1)d_1} \right) + \\
& + b_F \Bigg(\frac{c_d(1-h_1)d_1}{c_h h_1 + c_i(1-h_1)(1-d_1) + c_d(1-h_1)d_1} \frac{1}{c_f} + \\
& \quad + \frac{\frac{c_h h_1 c_{dh} d_2}{c_{dh}d_2 + c_{ih}(1-d_2)}}{c_h h_1 + c_i(1-h_1)(1-d_1) + c_d(1-h_1)d_1} \frac{1}{c_f} \Bigg) \Bigg]
\end{aligned}$$

To get the desired expression for the final size relation, let

$$\begin{aligned}\mathcal{R}_0 = b_I &\frac{1}{c_h h_1 + c_i(1-h_1)(1-d_1) + c_d(1-h_1)d_1} + \\ + b_H &\frac{\frac{c_h h_1}{c_{dh} d_2 + c_{ih}(1-d_2)}}{c_h h_1 + c_i(1-h_1)(1-d_1) + c_d(1-h_1)d_1} + \\ + b_F &\frac{\frac{c_d(1-h_1)d_1 + \frac{c_h h_1 c_{dh} d_2}{c_{dh} d_2 + c_{ih}(1-d_2)}}{c_f}}{c_h h_1 + c_i(1-h_1)(1-d_1) + c_d(1-h_1)d_1}\end{aligned} \tag{3.5}$$

and then we obtain

$$\log \frac{S_0}{S_\infty} = \left[1 - \frac{S_\infty}{N}\right] \mathcal{R}_0.$$

We claim that the expression (3.5) found for $\mathcal{R}_0$ is the reproduction number for the model (M3.1). When we evaluate (3.5) with the parameters from the paper [11], we obtain $\mathcal{R}_0 \approx 2.67$. This means that, at the beginning of the outbreak, one infectious individual yields on average 2.67 new infections during the duration of their infection.

3.1.2 Reproduction Number $\mathcal{R}_0$ - Advanced Derivation

As mentioned earlier, there is another, more rigorous way to compute the reproduction number. This method is described by P. van den Driessche and James Watmough in [9], or also again in [10]. For more details see these two papers. Note that we use the same notation as in the paper [9] for the following description. We will use the the same model (M3.1) as for the basic method for the demonstration.

For this method, we define two $(m \times 1)$ vectors $\boldsymbol{\mathcal{F}}$ and $\boldsymbol{\mathcal{V}}$, where m is the number of infectious compartments. For the Legrand model $m = 4$. Then, $\mathcal{F}_i$ is the rate of appearance of new infections in compartment i, and

$$\mathcal{V}_i = \mathcal{V}_i^- - \mathcal{V}_i^+,$$

where $\mathcal{V}_i^-$ denotes the rate of transfer of individuals out of the compartment i and $\mathcal{V}_i^+$ denotes the rate of transfer of individuals into the compartment i by all other means. The reproduction number $\mathcal{R}_0$ is then the spectral radius of $\mathbf{FV}^{-1}$, where

$$\mathbf{F} = \left.\frac{\partial \mathcal{F}_i}{\partial x_j}\right|_{x=x_0} \quad \text{and} \quad \mathbf{V} = \left.\frac{\partial \mathcal{V}_i}{\partial x_j}\right|_{x=x_0}, \text{ with } 1 \le i, j \le m.$$

For clarity, the compartments are sorted so that the first m compartments correspond to infectious compartments. Hence, $\mathbf{X} = (x_1, x_2, x_3, x_4, x_5, x_6) = (E, I, H, F, S, R)$. We assume $x_0 = (0, 0, 0, 0, N, 0)$ to be the disease free equilibrium. Note that x_0 is not unique, but it is customary to choose the one with the whole population susceptible.

The vectors $\boldsymbol{\mathcal{F}}$ and $\boldsymbol{\mathcal{V}}$ for the model (M3.1) are:

$$\boldsymbol{\mathcal{F}} = \begin{bmatrix} \frac{1}{N} b_I SI + \frac{1}{N} b_H SH + \frac{1}{N} b_F SF \\ 0 \\ 0 \\ 0 \end{bmatrix}$$

and

$$\boldsymbol{\mathcal{V}} = \begin{bmatrix} aE \\ -aE + [c_h h_1 + c_i(1-h_1)(1-d_1) + c_d(1-h_1)d_1]\, I \\ -c_h h_1 I + [c_{dh} d_2 + c_{ih}(1-d_2)]\, H \\ -c_d(1-h_1)d_1 I - c_{dh} d_2 H + c_f F \end{bmatrix}$$

It follows that,

$$\mathbf{F} = \begin{bmatrix} 0 & b_I & b_H & b_F \\ 0 & 0 & 0 & 0 \\ 0 & 0 & 0 & 0 \\ 0 & 0 & 0 & 0 \end{bmatrix}$$

and

$$\mathbf{V} = \begin{bmatrix} a & 0 & 0 & 0 \\ -a & c_h * h_1 + c_i * (1-h_1) * (1-d_1) + c_d * (1-h_1) * d_1 & 0 & 0 \\ 0 & -c_h * h_1 & c_{dh} * d_2 + c_{ih} * (1-d_2) & 0 \\ 0 & -c_d * (1-h_1) * d_1 & -c_{dh} * d_2 & c_f \end{bmatrix}$$

The spectral radius of $\mathbf{F}\mathbf{V}^{-1}$ is equal to the expression $\mathcal{R}_0$ found in 3.1.1 using the integration method. The computation was done in MATLAB and the code can be found in the Appendix B. Note that the reproduction number (3.5) found for the Lagrand model can be divided into three parts. Each part gives us the average yield of infections from the infectious compartments I, H, F respectively. We could use this information to determine which group contributes to the outbreak the most. Then, we can try to decrease that value by some means of intervention.

3.2 Example 2 - Eisenberg Multi-stage Ebola Model

As a second example of Ebola related model we chose a recent model from 2015 by M. Eisenberg, et al. [5]. We can think of it as an extension of the model from the Example 1. The main difference is that authors introduce two different stages of infectivity. The reason for it is that, at the beginning of an Ebola infection, a person shows just minor flu-like symptoms such as fever, joint and muscle pain, fatigue, etc. But after a certain period of time, the symptoms become more severe and that person becomes even more infectious. When the progress of Ebola gets to this stage the likelihood of surviving is very small. Group R_H represents people who already recovered but would still require a bed in a hospital.

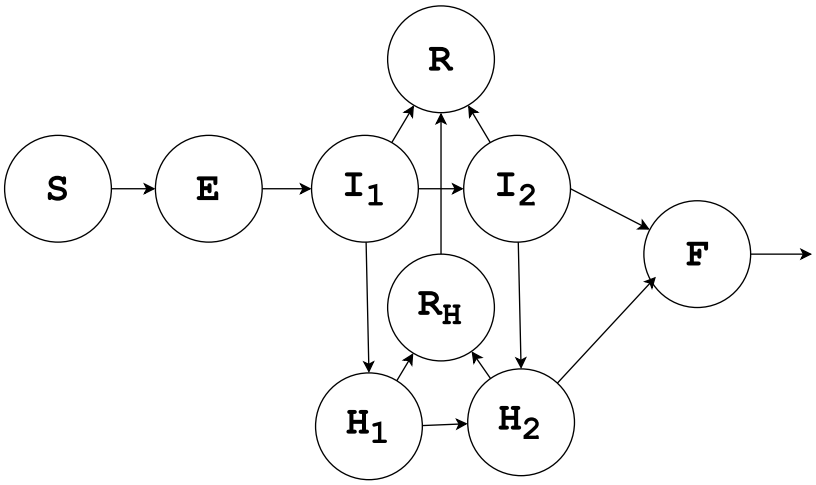

Figure 7: Flow chart of Eisenberg model.

For the sake of brevity, we will only depict the flow chart of this model. The system of differential equations, results, and information on all the parameters can be found in [5].

At this point we finished the introductory chapters and we will focus on the development of a new model. Our goal is to create a reasonable model, which could be used to model the transmission of Ebola. Then, we would like to discuss plausible ways to control the disease. Our advantage is that the most recent outbreak (2014-2015) in Africa is most likely over. Therefore, we can use the historical data to suggest what kind of interventions would have the greatest impact on the spread of the disease.

4 Models of Ebola Control

We developed a multicompartmental model based on the natural behavior of the disease and on the facts from previous outbreaks. The main focus was to incorporate the following control strategies into the model: hospitalization and safe burials. One of the main problems of the 2014-2015 outbreak in Africa was a limited number of beds in hospitals along with a lack of expertise of the medical workers. This led to a massive epidemic of Ebola mainly in three West African countries: Guinea, Liberia, and Sierra Leone. One of the WHO articles [6] aptly describes the situation in Liberia. "Basically no hospital anywhere in Liberia had an isolation ward. Few medical staff had been trained in the basic principles of infection prevention and control. Facilities had little or no personal protective equipment, not even gloves, and virtually no knowledge about how to use this equipment properly. Under such conditions, treatment of the first hospitalized patients ignited multiple chains of transmission, among staff, patients, and visitors, in ambulance and taxi drivers who ferried the sick to care, in relatives, neighbors, and eventually entire neighborhoods. Case numbers that had multiplied quickly began to grow exponentially". We can assume that a similar situations were true for the other two countries.

The outbreak started approximately in the summer 2014 and continued to spread significantly for about 200-250 days. After that, the disease got under control with only occasional cases from time to time. The following graphs depict the situation for the three countries.

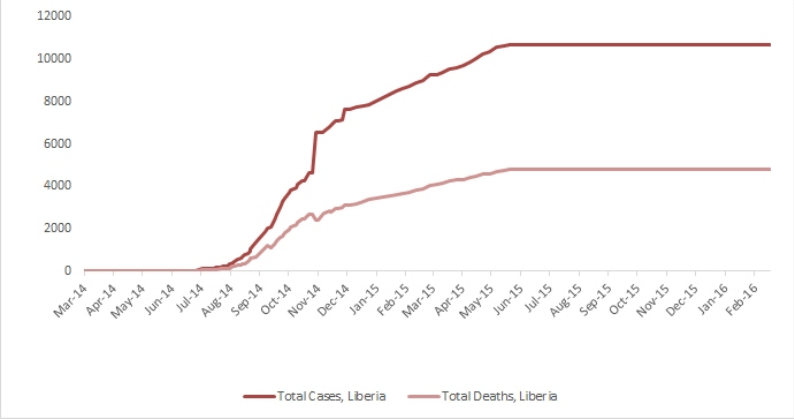

Figure 8: Cumulative cases of Ebola in Liberia in 2014-2015. The population of Liberia is 4.29 million. The mortality rate of people exposed to Ebola is 45.05%. *The country was declared Ebola free by WHO on May 9, 2015. [2], [7].*

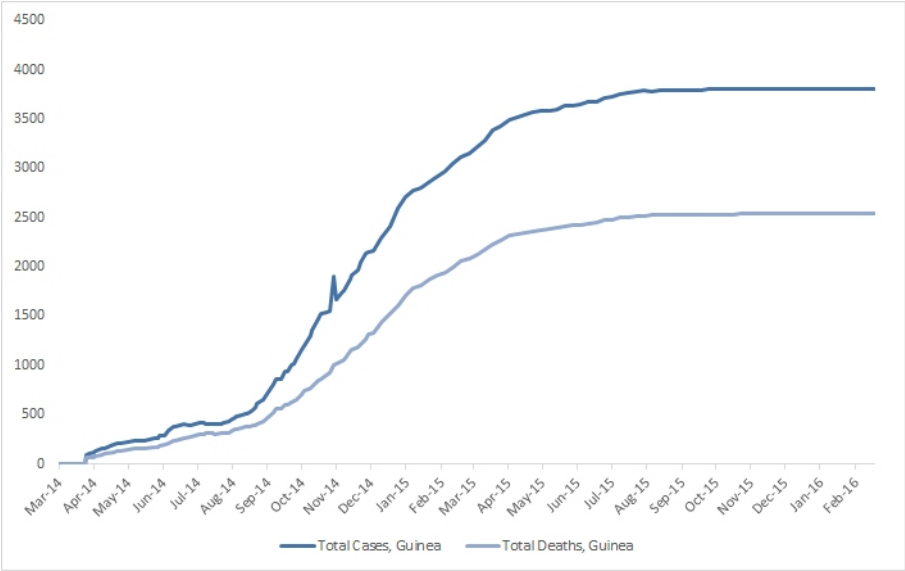

Figure 9: Cumulative cases of Ebola in Guinea in 2014-2015. The population of Guinea is 11.75 million. The mortality rate of people exposed to Ebola is 66.73%. *The country was declared Ebola free by WHO on December 29, 2015. [2], [7].*

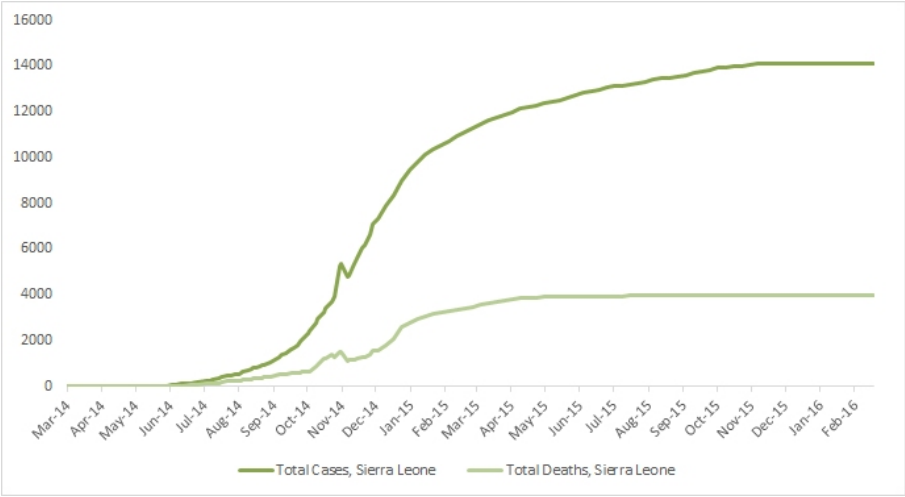

Figure 10: Cumulative cases of Ebola in Sierra Leone in 2014-2015. The population of Sierra Leone is 6.1 million. The mortality rate of people exposed to Ebola is 28.01%. *The country was declared Ebola free by WHO on November 7, 2015. [2], [7].*

An interesting fact can be observed around November 14, 2014. We can see a decrease in the number of cases even though the graphs show the cumulative numbers. This is due to imperfect case reporting and it illustrates how complicated the situation actually was. The lack of quarantine and troubles with localizing Ebola patients made the situation even more severe. As mentioned at the beginning, the deceased individuals were usually buried in a way of traditional customs for the certain country which resulted in a high risk of exposure for the people present at the funeral. One of the goals of the health organizations (such as CDC or WHO) was to inform people about the potential risks and to educate them to decrease the likelihood of the transmission.

Another important thing we can see from the graphs is the mortality rate of people exposed to Ebola. It significantly varies between the three countries and also over time. There are a couple possible explanations for this. One factor could be the initial level of medical care at the beginning of the outbreak. Another aspect could be the traditions and customs related to burials for certain areas as mentioned above. Lastly, the demographic structure of each country certainly plays a role.

A key role in fighting Ebola was the start of building more medical facilities, called Ebola Treatment Units (ETU). Safety procedures used in the ETUs provided the needed care which led to a decrease in spreading Ebola between staff in hospitals. In addition to that, there were medical (burial) teams working on the streets trying to locate individuals exposed to Ebola as well as performing safety burials of those who already died.

The main aim of this work is to show how these interventions might affect the epidemic of Ebola. Specifically, we consider an increase of the number of ETU beds as well as burial teams fighting the disease.

The first draft of our model is based on the following assumptions

- Population size N is assumed to be a constant
- The initial number of infectious people in the population is very small
- Mortality of those exposed to Ebola is approximately 50 % regardless of whether or not people are hospitalized
- We assume the same infective rates between infectious individuals who survive and those who do not
- We assume the same probability of hospitalization between the individuals who survive and those who do not
- Hospital size is unlimited
- Each non-hospital Ebola fatality is buried through the traditional burial
- People who recover from the disease receive permanent immunity

The first variant of our model does not include any limiting number of ETU beds or the presence of burial teams in the community. The model is described by the following differential equations:

$$
\begin{aligned}
\frac{\mathrm{d}S}{\mathrm{d}t} &= -\frac{1}{N}\left[\beta_{I_R} S I_R + \beta_{I_D} S I_D + \beta_{H_R} S H_R + \beta_{H_D} S H_D + \beta_F S F\right], \\
\frac{\mathrm{d}E}{\mathrm{d}t} &= \frac{1}{N}\left[\beta_{I_R} S I_R + \beta_{I_D} S I_D + \beta_{H_R} S H_R + \beta_{H_D} S H_D + \beta_F S F\right] - \alpha E, \\
\frac{\mathrm{d}I_R}{\mathrm{d}t} &= (1-\theta)\,\alpha E - (1-\pi)\epsilon_1 I_R - \pi\epsilon_2 I_R, \\
\frac{\mathrm{d}I_D}{\mathrm{d}t} &= \theta\alpha E - (1-\pi)\kappa_1 I_D - \pi\kappa_2 I_D, \\
\frac{\mathrm{d}H_R}{\mathrm{d}t} &= \pi\epsilon_2 I_R - \rho H_R, \\
\frac{\mathrm{d}H_D}{\mathrm{d}t} &= \pi\kappa_2 I_D - \delta H_D, \\
\frac{\mathrm{d}R}{\mathrm{d}t} &= (1-\pi)\epsilon_1 I_R + \rho H_R, \\
\frac{\mathrm{d}F}{\mathrm{d}t} &= (1-\pi)\kappa_1 I_D - \gamma F, \\
\frac{\mathrm{d}D}{\mathrm{d}t} &= \gamma F + \delta H_D.
\end{aligned}
\tag{M4.1}
$$

A better visualization of the model (M4.1) can be obtained from the flow chart shown below. The arrows represent the flow of individuals between the compartments.

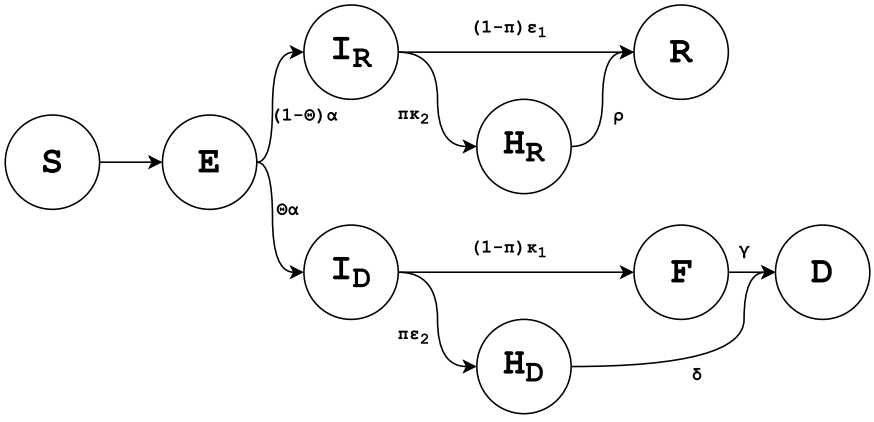

Figure 11: Flow chart of the developed model (M4.1). *The rough idea for this model came from combining two models from students' projects [15] and [16].*

The description of each of the compartments

S = susceptibles; people who can catch Ebola

E = people exposed to Ebola

I_R = infectious people who will recover

I_D = infectious people who pass away

H_R = hospitalized people who will recover

H_D = hospitalized people who will pass away

R = recovered individuals

F = non-hospitalized people waiting to be buried

D = deceased individuals

The main difference between our and other models from recent papers is that we divide the exposed population into two branches directly from the exposed class E, rather than doing that later on from the infectious or hospital classes. The split is based on the Ebola mortality at the given region. The individuals do not know in advance if they are going to survive or not, but since we know the probability of survival we can correspondingly use the information to determine their "destiny".

Another observation we made was that models from other papers yielded significantly bigger numbers of people who died from Ebola compared to the actual situation. This was usually due to the fact that the authors used the whole population of a certain country as a population at risk for catching the disease. But this assumption seems to be rather unrealistic. Clearly, people from different places do not interact with each other. Not even all people within one city interact with each other. Thus, our goal was to experiment with the population size to determine the effective population size. We decided to focus only on one county of Liberia: Montserrado, for which we were able to find enough of relevant information. It is the biggest county of Liberia with Liberia's capital, Monrovia, located there. The population of Montserrado is approximately 1.5 million. The initial parameters used for our model are shown in Table 1 below.

Parameters				
Parameter		Value	Units	Source
Population Size	N	1500000	people	[14], Estimated
Contact Rate - Community	β_{I_R}, β_{I_D}	0.160	people^{-1}days^{-1}	[13], Estimated
Contact Rate - Hospitals	β_{H_R}, β_{H_D}	0.062	people^{-1}days^{-1}	[13]
Contact Rate - Funerals	β_F	0.489	people^{-1}days^{-1}	[13]
Probability of Survival	$1-\theta$	0.54951	unitless	[7]
Incubation Period	α^{-1}	12.00	days	[13]
Time from Infection to Recovery	ϵ_1^{-1}	15	days	[13]
Time until Hospitalization	$\epsilon_2^{-1}, \kappa_2^{-1}$	3.24	days	[13]
Time from Infection to Death	κ_1^{-1}	13.31	days	[13]
Probability of Seeking Hospitalization	π	0.197	unitless	[13]
Time from Hospitalization to Recovery	ρ^{-1}	15.88	days	[13]
Time from Hospitalization to Death	δ^{-1}	10.07	days	[13]
Duration of Traditional Burial	γ^{-1}	2.01	days	[13]

Table 1: The description of parameters used in our model. Most of them were obtained from the paper [13] which deals directly with the outbreak in Liberia.

4.1 Analysis of the Model

At this moment we will perform an analysis of the model (M4.1) by finding the reproduction number and the final size relation. Once we introduce the desired interventions, the non-linearity of some of the terms will make it impossible to find these characteristics. We would like to find out if decreasing the population size can provide us with more accurate results. Our goal is not to produce a complete model, because our model still does not include important assumptions, but we want to focus on the effects of the presented interventions. However, we would still like to use reasonable parameter values, which yield results comparable to the general picture of the real situation.

By analogy to 3.1.2 the vectors $\boldsymbol{\mathcal{F}}$ and $\boldsymbol{\mathcal{V}}$ for the model (M4.1) in this section are:

$$\boldsymbol{\mathcal{F}} = \begin{bmatrix} \frac{1}{N}\beta_{I_R} SI_R + \frac{1}{N}\beta_{I_D} SI_D + \frac{1}{N}\beta_{H_R} SH_R + \frac{1}{N}\beta_{I_D} SH_D + \frac{1}{N}\beta_F SF \\ 0 \\ 0 \\ 0 \\ 0 \\ 0 \end{bmatrix}$$

and

$$\boldsymbol{\mathcal{V}} = \begin{bmatrix} \alpha E \\ -(1-\theta)\alpha E + (1-\pi)\epsilon_1 I_R + \pi\epsilon_2 I_R \\ -\theta\alpha E + (1-\pi)\kappa_1 I_D + \pi\kappa_2 I_D \\ -\pi\epsilon_2 I_R + \rho H_R \\ -\pi\kappa_2 I_D + \delta H_D \\ (1-\pi)\kappa_1 I_D - \gamma F \end{bmatrix}$$

Note that $\mathbf{X} = (E, I_R, I_D, H_R, H_D, F, S, R, D)$ and the disease free equilibrium is analogously $x_0 = (0, 0, 0, 0, 0, 0, N, 0, 0)$. It follows that the matrices $\mathbf{F}$ and $\mathbf{V}$ for our model are:

$$\mathbf{F} = \begin{bmatrix} 0 & \beta_{I_R} & \beta_{I_D} & \beta_{H_R} & \beta_{H_D} & \beta_F \\ 0 & 0 & 0 & 0 & 0 & 0 \\ 0 & 0 & 0 & 0 & 0 & 0 \\ 0 & 0 & 0 & 0 & 0 & 0 \\ 0 & 0 & 0 & 0 & 0 & 0 \\ 0 & 0 & 0 & 0 & 0 & 0 \end{bmatrix}$$

$$\mathbf{V} = \begin{bmatrix} \alpha & 0 & 0 & 0 & 0 & 0 \\ -(1-\theta)*\alpha & (1-\pi)\epsilon_1 + \pi*\epsilon_2 & 0 & 0 & 0 & 0 \\ -\theta*\alpha & 0 & (1-\pi)\kappa_1 + \pi*\kappa_2 & 0 & 0 & 0 \\ 0 & -\pi*\epsilon_2 & 0 & \rho & 0 & 0 \\ 0 & 0 & -\pi*\kappa_2 & 0 & \delta & 0 \\ 0 & 0 & -(1-\pi)\kappa_1 & 0 & 0 & \gamma \end{bmatrix}$$

The spectral radius of $\mathbf{FV}^{-1}$ yields

$$\begin{aligned} &\mathcal{R}_0 = \mathcal{R}_0^1 + \mathcal{R}_0^2 + \mathcal{R}_0^3 + \mathcal{R}_0^4 + \mathcal{R}_0^5, \\ &\mathcal{R}_0 = \frac{(1-\theta)\beta_{I_R}}{(1-\pi)\epsilon_1 + \pi\epsilon_2} + \frac{\theta\beta_{I_D}}{(1-\pi)\kappa_1 + \pi\kappa_2} + \\ &\quad + \frac{(1-\theta)\beta_{H_R}\pi\epsilon_2}{\rho((1-\pi)\epsilon_1 + \pi\epsilon_2)} + \frac{\theta\beta_{H_D}\pi\kappa_2}{\delta((1-\pi)\kappa_1 + \pi\kappa_2)} + \frac{\theta\beta_F(1-\pi)\kappa_1}{\gamma((1-\pi)\kappa_1 + \pi\kappa_2)} \end{aligned} \tag{4.1}$$

Evaluating the reproduction number (4.1) using the parameters from Table 1 gives us $\mathcal{R}_0 = 2.013$. The following table tells us how much each infectious group contributes to the spread of the disease.

i	Group	$\mathcal{R}_0^i$
1	Infectious compartment, to recover (I_R)	0.7690
2	Infectious compartment, to die (I_D)	0.5950
3	Hospital compartment, to recover (H_R)	0.2877
4	Hospital compartment, to die (H_D)	0.1412
5	Funeral compartment (F)	0.2205

Table 2: Reproduction number of each infective group.

Since there are few other analytical tools to analyze this model, we will focus on numerical simulations using computer software (Mathematica, Matlab). Firstly, we will run the simulation of the whole model and plot the solutions over a certain time interval. The following graph shows the simulation of our system with initial conditions $S_0 = N - E_0$ and $E_0 = 32$. Other compartments are initially zero.

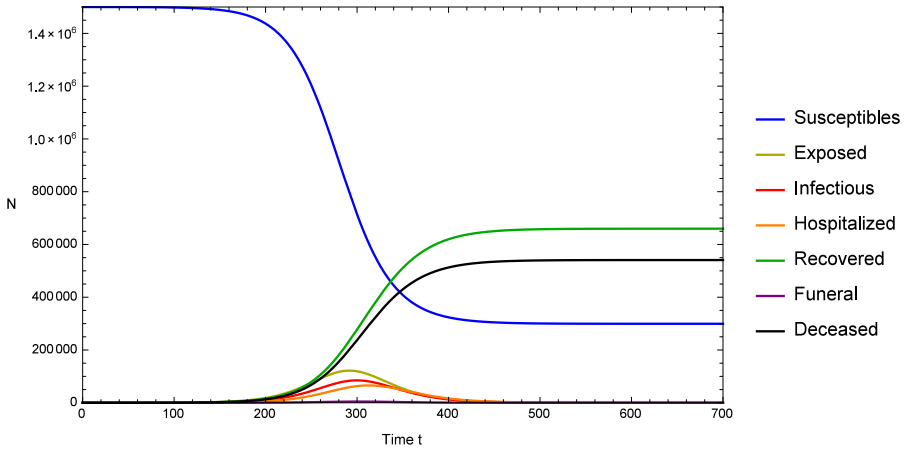

Figure 12: Numerical simulation of the model (M4.1)*, with the parameters from Table 1 and $S_0 = N - E_0$ and $E_0 = 32$. The graph shows long term behavior over 700 days. We can see the progress of the outbreak through each of the compartments. Note that the typical pulse pattern as described for the SIR model is present. However, it seems like even though we focus only on one specific region, the size of N is still too big. The prediction from our model is nowhere near to the actual number of people exposed to Ebola or the duration of the outbreak.*

Remark 4.1. The initial time for this simulation is taken to be July 1, 2014 based on the information found in [8]. The initial number of hospital beds in Montserrado county was less than 100 and after 20 days the first of a total of 4 ETUs started to be built. They reached a peak of ETU size around 80 days after July 1 with roughly 500 beds. It was claimed that more than a 1,000 beds were needed [14]. The main portion of the outbreak lasted for 200-250 days. ETU bed limitation will be included later on in our advanced model.

4.2 Fitting of the Model to the Data

As a measure of the predictive accuracy of our models, we add a cumulative function of people exposed to Ebola given by the following equation to the model (M4.1)

$$I_c^t = \int_0^t \alpha E(\tau)\, d\tau \tag{4.2}$$

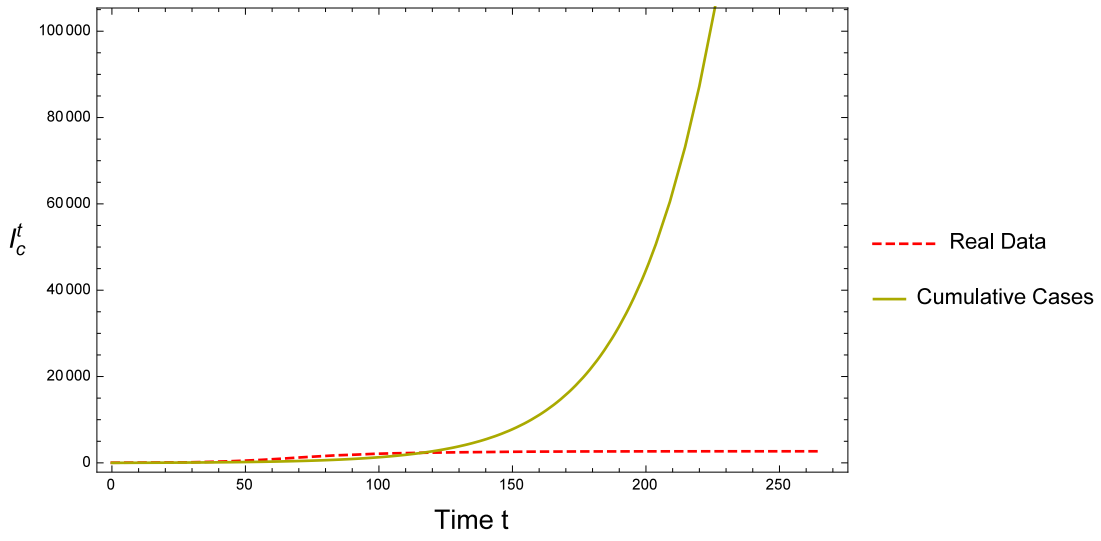

Figure 13: Figure depicts (the dashed line) the real cumulative cases of Ebola in Montserrado county during the 2014-2015 outbreak [8]. The solid line is the prediction from the model (M4.1)*, with parameters from Table 1. The result likely suggests that the population at risk is actually significantly smaller than the actual population size N.*

We used numerical simulations to experiment with the population size N. Based on the information from Table 2, we know that the main source of new infections is from the non-hospitalized infectious population from compartments I_R and I_D. Hence, we

also vary these in the hope of obtaining better results. Figure 14 depicts the resulting parameter fitting.

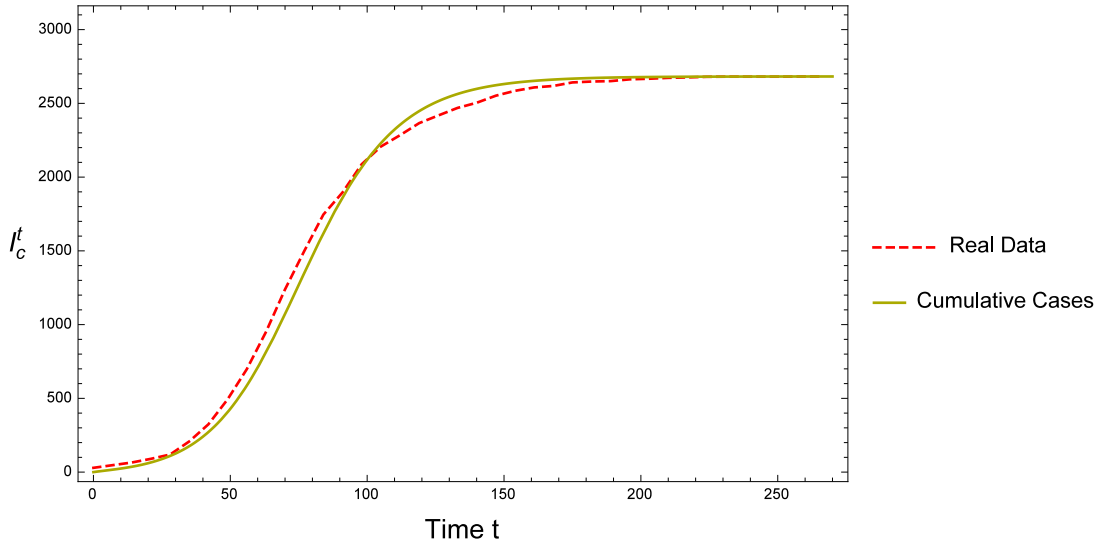

Figure 14: We can see a very close match of the model (M4.1) *with the real data. The new parameter values are* $N = 2860$ *and* $\beta_{I_R}, \beta_{I_D} = 0.27$. *(Table 3)*

Remark 4.2. The new size of the population $N = 2860$ is significantly smaller than the original one. It actually seems to make sense, because if we look at the real data, even though the outbreak was enormous by historical standards, "only" 0.249% were exposed to Ebola in Liberia. We also slightly increased the community contact rates β_{I_R} and β_{I_D} from 0.16 to 0.27 to match the steeper exponential growth of the disease.

Updated Parameters			
Parameter	Value	Units	Source
Population Size N	2860	people	Estimated
Contact Rate - Community β_{I_R}, β_{I_D}	0.270	$\text{people}^{-1}\text{days}^{-1}$	Estimated

Table 3: The list of updated parameters after visual fitting. We varied the population size N *and the community contact rates* β_{I_R} *and* β_{I_D}.

4.3 Modeling Ebola Control Strategies

4.3.1 Limited Number of Hospital Beds

To make our model more realistic we have to consider that hospitals (or ETUs) have limited sizes. Based on the information found in [14], there were 4 ETUs built in Montserrado county (Liberia) between 20th-80th day of the outbreak. This increased the number of hospital beds from 100 to 500. The officials claimed that there was a significant shortage of beds at the beginning of the outbreak (more than 1,000 beds needed). For simplicity, we assume that number of beds is equally distributed between the ETUs and that they are spread over the region, so that an individual seeking help can go only to one of them per day. This means that the number of hospital beds is effectively divided by 4. Also, we know that many people who came to the ETUs did not have Ebola, although they would still occupy a bed until the tests confirmed that. These tests usually took 2-5 days. As described in [14] (and shown in Figure 15), the proportion of non-Ebola patients varies significantly over time. However, for simplicity we will assume it was constant. We denote the ratio of Ebola patience versus all patients by μ and we estimate it to be the mean of actual data, $\mu = 0.85$.

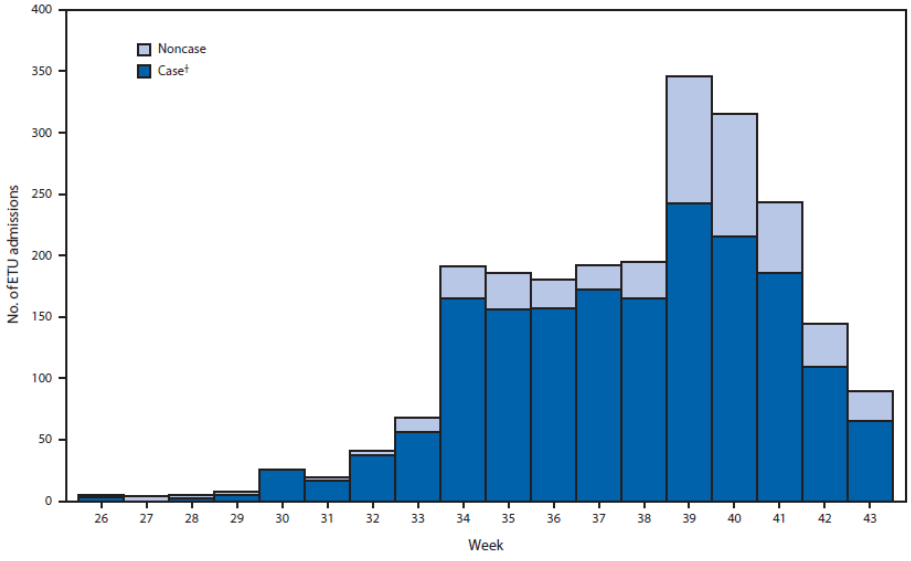

Figure 15: The cases admitted to ETUs during the Liberia epidemic in Montserrado county. [14] The starting date of our simulation, July 1, represents week 27 in the picture. We use the data to estimate a constant average number of people admitted to ETUs who tested negative for Ebola.

The way we modeled the limited size of ETUs is the following. Hospitals with available beds are being filled by incoming patients at the same rate as in our initial model (M4.1). Recall that the rates are $\pi\epsilon_2 I_R$ and $\pi\kappa_2 I_D$. Once the hospital reaches its maximum capacity, there are two options. If the number of people trying to get into a hospital is higher than the rate out of the hospital, then some individuals cannot be accepted and the rate of admission is set to be equal to the rate at which beds become available. A way to model this is to decrease the probability of seeking hospitalization π (note that it is assumed to be the same for both recovery and death divisions of our model). Let us denote this new decreased probability of seeking hospitalization by $\Pi(t)$.

The decreased $\Pi(t)$ is designed, so that the rate of change of the hospital class is zero when the hospital is full. In other words, $(H_R'(t) + H_D'(t)) = 0$. The new rates of full hospital admission are:

$$\begin{aligned}&\text{Recovery division: } \Pi(t)\epsilon_2 I_R,\\ &\text{Death division: } \Pi(t)\kappa_2 I_D,\end{aligned}$$

where $\Pi(t) = \dfrac{\rho H_R + \delta H_D}{\epsilon_2 I_R + \kappa_2 I_D}$.

Remark 4.3. Note that the updated probability of hospitalization

$$\Pi(t) = \frac{\rho H_R + \delta H_D}{\epsilon_2 I_R + \kappa_2 I_D} \tag{4.3}$$

describes the ratio of people leaving the hospitals versus the people available to go to the hospital. For the sake of brevity we will denote this fraction by $\Pi(t) = \Pi$.

When the number of people trying to get in drops and the hospital frees some beds, then the rate of admission becomes again $\pi\epsilon_2 I_R$ and $\pi\kappa_2 I_D$, respectively. We model this with a switch between π and Π based on if the hospital is full.

It is important to say that the change from $\pi \to \Pi$ results in a bigger portion of people staying in the non-hospitalized infectious classes who recover/die on their own. We must correspondingly adjust that proportion as well. We will use an additional switch between $(1-\pi)$ and $(1-\Pi)$. Note that both switches must be triggered simultaneously. The rates of recovery/death for non-hospitalized are then:

$$\begin{aligned}&\text{Recovery division: } (1-\pi)\epsilon_1 I_R \quad \text{or} \quad (1-\Pi)\epsilon_1 I_R,\\ &\text{Death division: } (1-\pi)\kappa_1 I_D \quad \text{or} \quad (1-\Pi)\kappa_1 I_D,\end{aligned}$$

respectively.

Let us introduce a new term H_{max} which will denote the maximum number of hospital beds. For simplicity we assume that the number of beds is constant even though we found the information about when each ETU in Montserrado county was built. This is justified by numerical experiments which showed that the results were practically the same whether H_{max} was time dependent or just a fixed number. The benefit of this is that the numerical simulations are faster. We experienced significant numerical issues with the time changing H_{max} because the system became stiff.

The way we modeled the described approach was to use **If** functions along with **Minimum** and **Maximum** functions in Mathematica. The changes to the equations are the following (we use Mathematica syntax for the description):

$$
\begin{aligned}
\frac{\mathrm{d}S}{\mathrm{d}t} &= -\frac{1}{N}\left[\beta_{I_R} S I_R + \beta_{I_D} S I_D + \beta_{H_R} S H_R + \beta_{H_D} S H_D + \beta_F S F\right], \\
\frac{\mathrm{d}E}{\mathrm{d}t} &= \frac{1}{N}\left[\beta_{I_R} S I_R + \beta_{I_D} S I_D + \beta_{H_R} S H_R + \beta_{H_D} S H_D + \beta_F S F\right] - \alpha E, \\
\frac{\mathrm{d}I_R}{\mathrm{d}t} &= (1-\theta)\alpha E - \mathrm{If}\left[(H_R + H_D) < \mu H_{max}, (1-\pi)\epsilon_1 I_R + \pi\epsilon_2 I_R,\right. \\
&\quad \left.\mathrm{Max}\left[(1-\Pi)\,\epsilon_1 I_R, (1-\pi)\epsilon_1 I_R\right] + \mathrm{Min}\left[\Pi\epsilon_2 I_R, \pi\epsilon_2 I_R\right]\right], \\
\frac{\mathrm{d}I_D}{\mathrm{d}t} &= \theta\alpha E - \mathrm{If}\left[(H_R + H_D) < \mu H_{max}, (1-\pi)\kappa_1 I_D + \pi\kappa_2 I_D,\right. \\
&\quad \left.\mathrm{Max}\left[(1-\Pi)\,\kappa_1 I_D, (1-\pi)\kappa_1 I_D\right] + \mathrm{Min}\left[\Pi\kappa_2 I_D, \pi\kappa_2 I_R\right]\right], \\
\frac{\mathrm{d}H_R}{\mathrm{d}t} &= \mathrm{If}\left[(H_R + H_D) < \mu H_{max}, \pi\epsilon_2 I_R, \mathrm{Min}\left[\Pi\epsilon_2 I_R, \pi\epsilon_2 I_R\right]\right] - \rho H_R, \\
\frac{\mathrm{d}H_D}{\mathrm{d}t} &= \mathrm{If}\left[(H_R + H_D) < \mu H_{max}, \pi\kappa_2 I_D, \mathrm{Min}\left[\Pi\kappa_2 I_D, \pi\kappa_2 I_D\right]\right] - \delta H_D, \\
\frac{\mathrm{d}R}{\mathrm{d}t} &= \mathrm{If}\left[(H_R + H_D) < \mu H_{max}, (1-\pi)\epsilon_1 I_R, \mathrm{Max}\left[(1-\Pi)\,\epsilon_1 I_R, (1-\pi)\epsilon_1 I_R\right]\right] + \rho H_R, \\
\frac{\mathrm{d}F}{\mathrm{d}t} &= \mathrm{If}\left[(H_R + H_D) < \mu H_{max}, (1-\pi)\kappa_1 I_D, \mathrm{Max}\left[(1-\Pi)\,\kappa_1 I_D, (1-\pi)\kappa_1 I_D\right]\right] - \gamma F, \\
\frac{\mathrm{d}D}{\mathrm{d}t} &= \gamma F + \delta H_D.
\end{aligned}
\tag{M4.2}
$$

Note that the equations for S, E, and D remain the same as in the model (M4.1). Rather than fitting this model to the real data again, our intentions are to find out how effectively we can influence the outbreak by increasing the number of hospital beds. To

do this we plot the cumulative function I_c^t, given by (4.2), at the time $t = 500$ (after the outbreak is over) as a function of the number of hospital beds H_{max}. The results are depicted in the graph below.

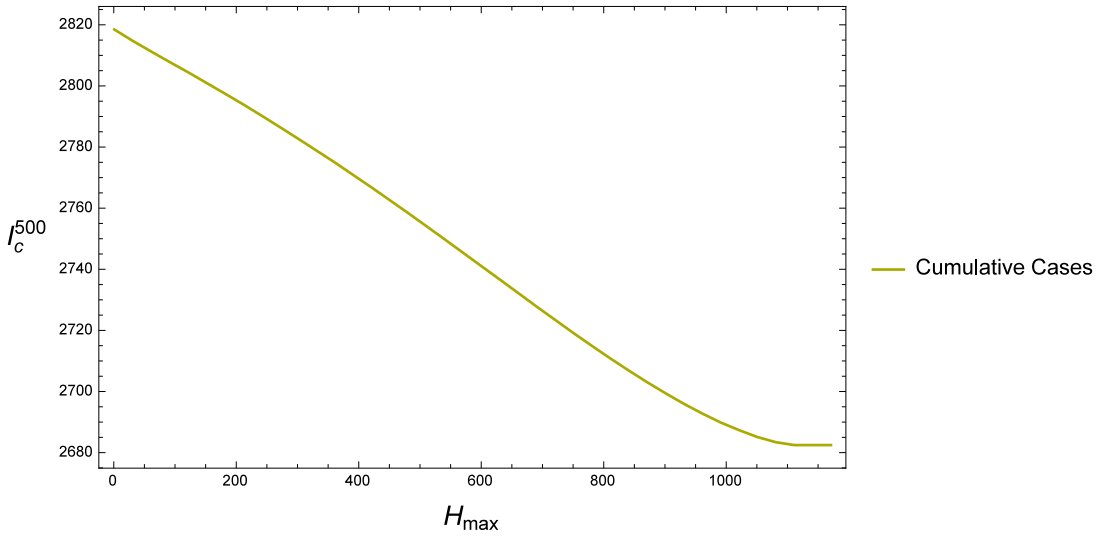

Figure 16: The graph shows the function I_c^t of the model (M4.2) *at time $t = 500$ as a function of combined hospitals/ETUs size (the number of beds H_{max}). The parameter values used for this model are in Table 1 updated by Table 3, with $\mu = 0.85$.*

We can see that as we increase the number of beds the total cases decrease steadily until we reach approximately $1,100$ of beds. From a disease control point of view, having more than $1,000$ beds does not make sense because they would never fill up anyway. Recall that the report [14] claimed that over $1,000$ of beds were needed during the peak period. The result from our model predicts $1,100$ beds needed. Note that the result is influenced by our estimation of the fraction μ of hospital beds actually available to Ebola patients, $0 \leq \mu \leq 1$. μH_{max} represents the effective hospital size.

We conclude from our model that Montserrado county with a population of 1.5 million requires roughly over $1,100$ beds to effectively fight the disease. Anything more than that would be a waste of resources. With large hospital capacity, 93.81 % of the susceptible population is infected by Ebola, but with no hospitals at all the ration increases to 98.57 %. Note that the percentages are related to a hypothetical community of reduced size $N = 2860$, rather than the whole population of Montserrado county.

4.3.2 Modeling Burial Teams

To continue the discussion of various Ebola control strategies we describe the effect of burial teams. In our model the teams help with safety burials, and therefore decrease the transmission of Ebola from the F (funeral) compartment. At this point, we do not take into account that the teams can inform people, distribute health kits with basic medical equipment, or encourage more people to go seek help or get tested in ETUs. These factors might also influence the disease dynamic and some will be considered in the next section of this chapter.

The way we modeled the effect of burial teams is the following.

$$\begin{aligned}
\frac{\mathrm{d}S}{\mathrm{d}t} &= -\frac{1}{N}\left[\beta_{I_R} S I_R + \beta_{I_D} S I_D + \beta_{H_R} S H_R + \beta_{H_D} S H_D + \beta_F S F\right], \\
\frac{\mathrm{d}E}{\mathrm{d}t} &= \frac{1}{N}\left[\beta_{I_R} S I_R + \beta_{I_D} S I_D + \beta_{H_R} S H_R + \beta_{H_D} S H_D + \beta_F S F\right] - \alpha E, \\
\frac{\mathrm{d}I_R}{\mathrm{d}t} &= (1-\theta)\,\alpha E - (1-\pi)\epsilon_1 I_R - \pi\epsilon_2 I_R, \\
\frac{\mathrm{d}I_D}{\mathrm{d}t} &= \theta\alpha E - (1-\pi)\kappa_1 I_D - \pi\kappa_2 I_D, \\
\frac{\mathrm{d}H_R}{\mathrm{d}t} &= \pi\epsilon_2 I_R - \rho H_R, \\
\frac{\mathrm{d}H_D}{\mathrm{d}t} &= \pi\kappa_2 I_D - \delta H_D, \\
\frac{\mathrm{d}R}{\mathrm{d}t} &= (1-\pi)\epsilon_1 I_R + \rho H_R, \\
\frac{\mathrm{d}F}{\mathrm{d}t} &= \kappa_1 I_D - \gamma F - \mathcal{T}\frac{f_1 F}{\frac{f_1}{f_2} + F}, \\
\frac{\mathrm{d}D}{\mathrm{d}t} &= \gamma F + \mathcal{T}\frac{f_1 F}{\frac{f_1}{f_2} + F}
\end{aligned} \tag{M4.3}$$

Note that the only difference from the model (M4.1) is in equations for F and D. These equations are modified with the Holling Type-II functional response term. The parameter $\mathcal{T}$ denotes the number of burial teams and f_1 represents the maximum number of bodies that can be buried per day. The ratio $\frac{f_1}{f_2}$ is the so-called half saturation constant. It tells us how many bodies would set the burial teams to half of their maximum performance. Specifically, the teams are burying the bodies, but if there are very few people to bury, they spend more time searching for them.

We were not able to find exact information about how many teams were working on the streets and how many bodies they could possibly bury per day. We decided to vary the number of teams from $0 - 40$ with $f_1 = 1$ and $f_1/f_2 = 2$. These values might seem rather low, but we have to consider that the teams are spread around the whole county. This is analogous to limited ETU size, where H_{max} was divided by 4 to effectively distribute the hospital beds among the four ETUs built in Montserrado.

As with hospital size, we produce the following graph:

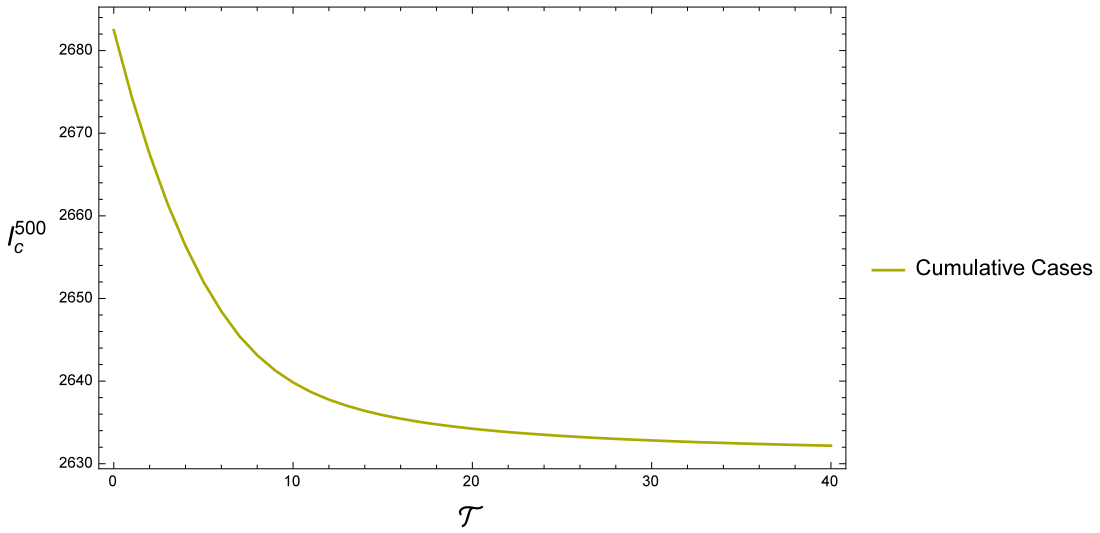

Figure 17: The graph shows the function I_c^t of the model (M4.3) *at time $t = 500$ as a function of the number of burial teams $\mathcal{T}$. The parameter values used for this model are in Table 1 updated by Table 3.*

We observe a differently shaped effect on the Ebola dynamics in Figure 17 compared to the analogous result with limited number of ETU beds in Figure 16. There is a rapid decrease between $0 - 20$ teams and then the influence of more teams becomes less significant. If we assume that each team consist of 10 people, then having 20 teams means 200 workers total. Even though we could not find any precise information, this number seems to be believable. From a control point of view, these results suggest not to increase the number of teams to more than 20 to ensure a reasonable performance/cost effectiveness.

4.3.3 Combining Limited Hospital Size and Burial Teams

In order to measure the combined effects of larger hospital sizes and burial teams we will combine the two approaches from sections 4.3.1 and 4.3.2. The resulting system of differential equations is the following. The goal is to distinguish between the effects of these two interventions and to determine the best combination which results in the highest decrease of Ebola transmission while also saving as many resources as possible.

$$
\begin{aligned}
\frac{\mathrm{d}S}{\mathrm{d}t} &= -\frac{1}{N}\left[\beta_{I_R} S I_R + \beta_{I_D} S I_D + \beta_{H_R} S H_R + \beta_{H_D} S H_D + \beta_F S F\right], \\
\frac{\mathrm{d}E}{\mathrm{d}t} &= \frac{1}{N}\left[\beta_{I_R} S I_R + \beta_{I_D} S I_D + \beta_{H_R} S H_R + \beta_{H_D} S H_D + \beta_F S F\right] - \alpha E, \\
\frac{\mathrm{d}I_R}{\mathrm{d}t} &= (1-\theta)\alpha E - \mathrm{If}\left[(H_R + H_D) < \mu H_{max}, (1-\pi)\epsilon_1 I_R + \pi\epsilon_2 I_R,\right. \\
&\quad \left.\mathrm{Max}\left[(1-\Pi)\,\epsilon_1 I_R, (1-\pi)\epsilon_1 I_R\right] + \mathrm{Min}\left[\Pi\epsilon_2 I_R, \pi\epsilon_2 I_R\right]\right], \\
\frac{\mathrm{d}I_D}{\mathrm{d}t} &= \theta\alpha E - \mathrm{If}\left[(H_R + H_D) < \mu H_{max}, (1-\pi)\kappa_1 I_D + \pi\kappa_2 I_D,\right. \\
&\quad \left.\mathrm{Max}\left[(1-\Pi)\,\kappa_1 I_D, (1-\pi)\kappa_1 I_D\right] + \mathrm{Min}\left[\Pi\kappa_2 I_D, \pi\kappa_2 I_R\right]\right], \\
\frac{\mathrm{d}H_R}{\mathrm{d}t} &= \mathrm{If}\left[(H_R + H_D) < \mu H_{max}, \pi\epsilon_2 I_R, \mathrm{Min}\left[\Pi\epsilon_2 I_R, \pi\epsilon_2 I_R\right]\right] - \rho H_R, \\
\frac{\mathrm{d}H_D}{\mathrm{d}t} &= \mathrm{If}\left[(H_R + H_D) < \mu H_{max}, \pi\kappa_2 I_D, \mathrm{Min}\left[\Pi\kappa_2 I_D, \pi\kappa_2 I_D\right]\right] - \delta H_D, \\
\frac{\mathrm{d}R}{\mathrm{d}t} &= \mathrm{If}\left[(H_R + H_D) < \mu H_{max}, (1-\pi)\epsilon_1 I_R, \mathrm{Max}\left[(1-\Pi)\,\epsilon_1 I_R, (1-\pi)\epsilon_1 I_R\right]\right] + \rho H_R, \\
\frac{\mathrm{d}F}{\mathrm{d}t} &= \mathrm{If}\left[(H_R + H_D) < \mu H_{max}, (1-\pi)\kappa_1 I_D, \mathrm{Max}\left[(1-\Pi)\,\kappa_1 I_D, (1-\pi)\kappa_1 I_D\right]\right] - \gamma F - NT\frac{f_1 F}{\frac{f_1}{f_2} + F}, \\
\frac{\mathrm{d}D}{\mathrm{d}t} &= \gamma F + NT\frac{f_1 F}{\frac{f_1}{f_2} + F}.
\end{aligned}
\tag{M4.4}
$$

Recall that $\Pi = \dfrac{\rho H_R + \delta H_D}{\epsilon_2 I_R + \kappa_2 I_D}$ as given by (4.3).

We will again measure the effect of the two interventions by plotting the total number of people exposed to Ebola measured at the end of the outbreak ($t = 500$).

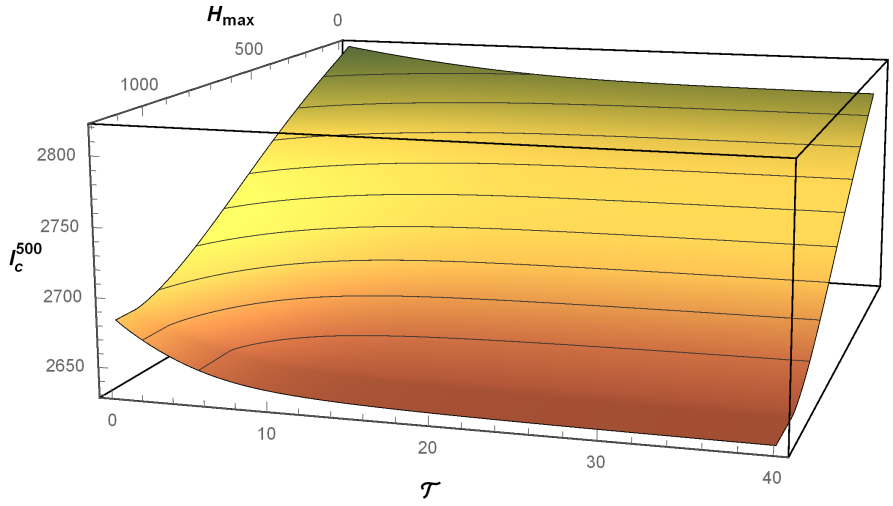

Figure 18: The graph shows the function I_c^t of the model (M4.4) *at time $t = 500$ as a function of the number of hospital beds H_{max} and the number of burial teams $\mathcal{T}$. The parameter values used for this model are in Table 1 updated by Table 3, with $\mu = 0.85$.*

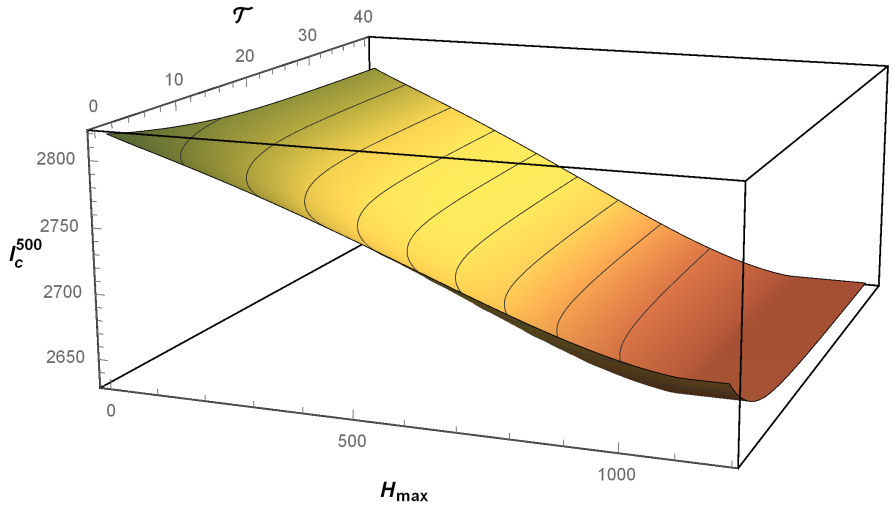

Figure 19: Same as the previous figure but from a different angle.

For better understanding of the two previous 3D plots, we will depict a contour plot.

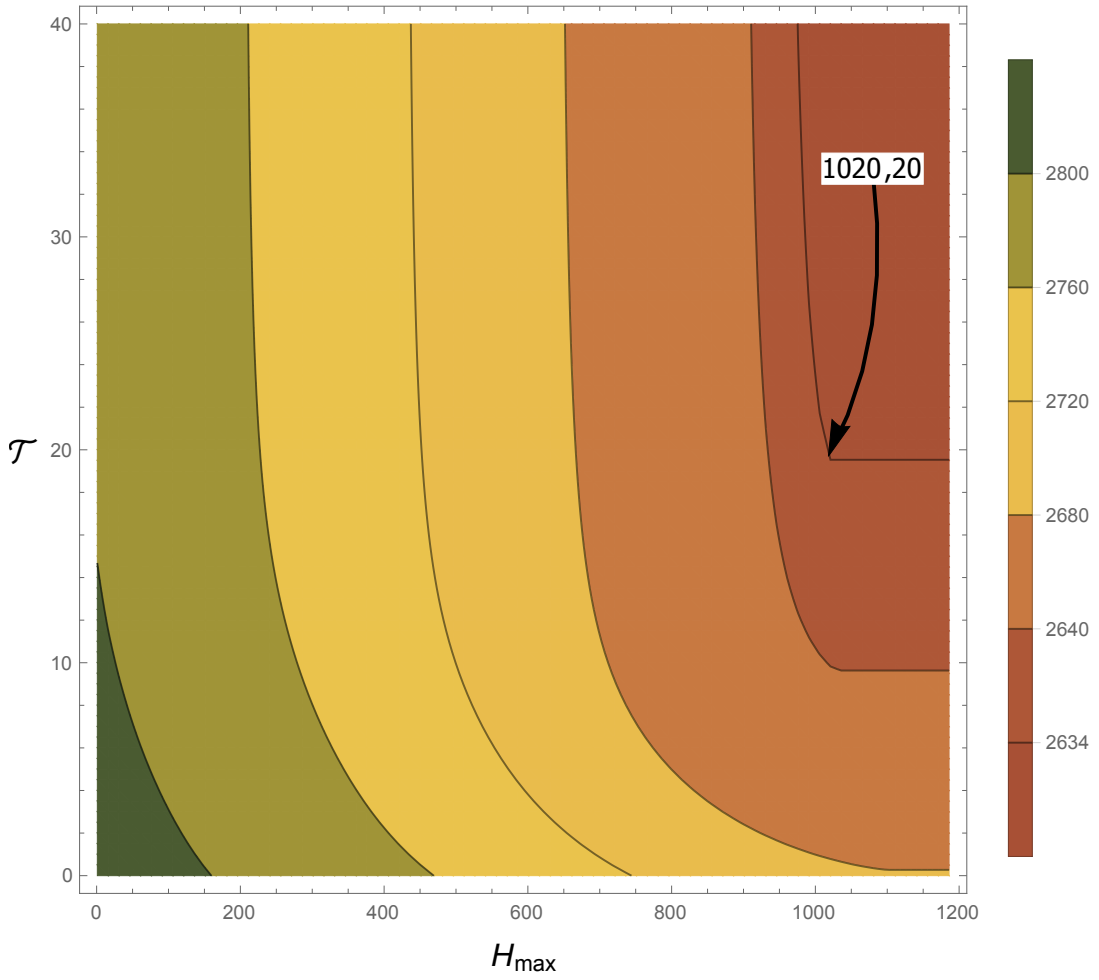

Figure 20: The contour plot version of the previous two graphs.

Remark 4.4. By looking at the last Figure we choose the most effective control to be in the top right region (contour level equals to 2634). For $I_c^t = 2634$ an optimal solution was observed to be 20 burial teams and roughly 1020 beds. This would be our suggestion for officials responsible for the chosen county to use their resources reasonably. Using the resources to create these numbers of beds and teams would result in approximately $2,634$ Ebola cases in the population of Montserrado.

For curiosity, we are interested in fixing the number of beds and burial teams to the values mentioned in the Remark 4.4 and plotting the cumulative Ebola cases along with the real data [8].

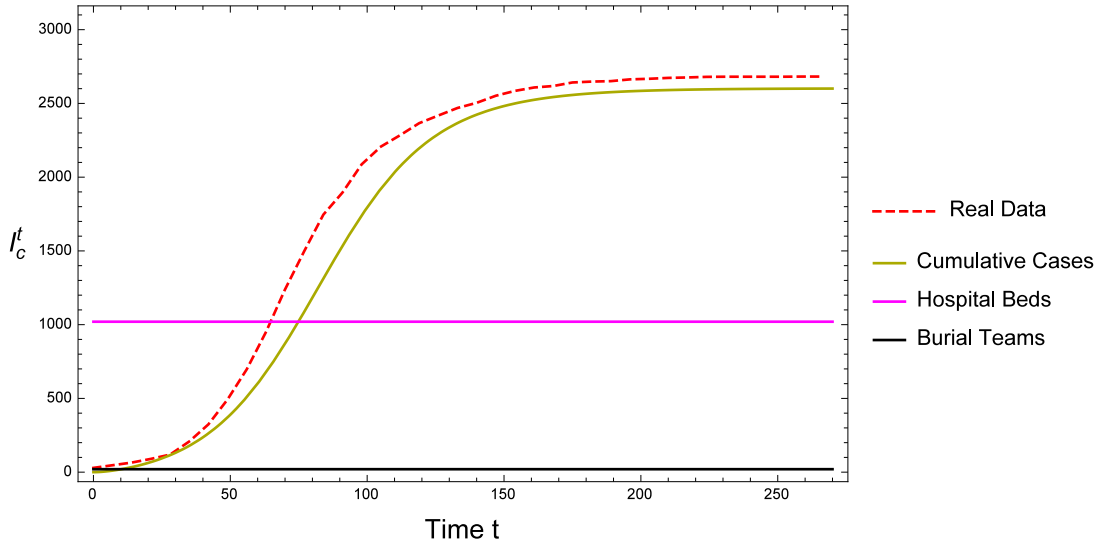

Figure 21: The graph of I_c^t of the model (M4.4)*, with fixed number of burial teams $\mathcal{T} = 20$ and hospital beds $H_{max} = 1020$ for the Montserrado county over time. The dashed line depicts the real data [8]. The parameter values used for this model are in Table 1 updated by Table 3, with $\mu = 0.85$.*

It is not a surprise that we see our model predicting fewer people catching Ebola compared to the real situation. This was our control goal from the beginning. We intended to model the medical interventions which were actually implemented by the local government and international health organizations. However, we observe only a slight improvement. This is because through the used interventions we modified the hospital and funeral transmissions. Although, the most significant contribution of the Ebola transmission is from the infectious classes (infectious people who are alive but not in the hospitals). Thus, reducing the contact rates β_{I_R} and β_{I_D} would affect the outcome of the outbreak the most. This could be done through quarantine and distribution of surgical masks and gloves. But if this was actually possible, then there probably would not be an outbreak at all or it would be at least at a significantly smaller scale.

4.3.4 Modeling Increased Probability of Seeking Hospitalization

The last question we asked ourselves was how an increased desire for hospitalization would affect the dynamic of the epidemic. This means to increase the parameter π. Recall that this parameter was estimated to be $\pi = 0.197$ which means that nearly 20 % of people exposed to Ebola try to go to an ETU.

We justify changing the value of π by knowing that there were medical teams working on the streets which could send individuals to hospitals. Our approach was the following. We assumed that the parameter π is dependent on the number of burial teams present in the community. However, it is difficult to guess any specific relationship. Hence, we will fix the number of hospital beds and burial teams to be the optimal values found in the previous section: $H_{max} = 1020$ and $\mathcal{T} = 20$, respectively. Then, we will produce the same kind of plot as in Figures 16 and 17.

After running the simulations, we discovered very interesting behavior. Increased probability of hospitalization resulted in significantly lesser Ebola transmissions as well as delayed the outbreak. The hospitals filled up almost at the same pace but they would stay full for longer period of time. The main significance of that change was mainly at the beginning of the epidemic which resulted in lesser consequences of Ebola crises. The effect of increasing π was small when the number of beds was small, but with a large ETU capacity, the effect was enormous.

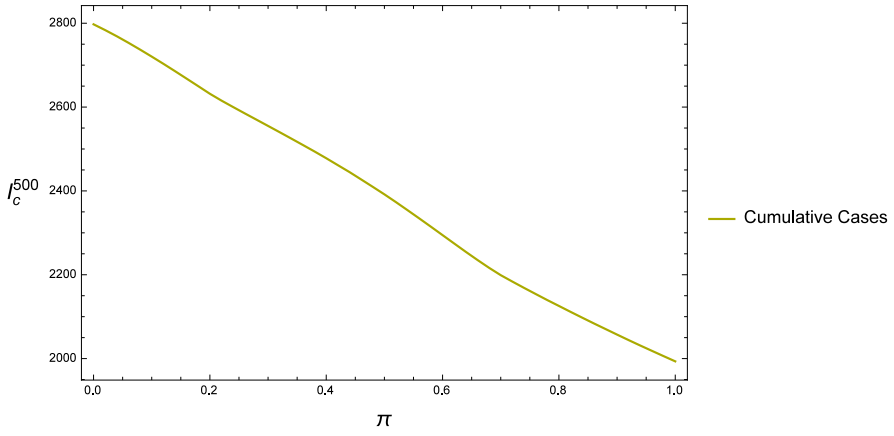

Figure 22: The graph shows the function (4.2) I_c^t *of the model* (M4.4) *at time* $t = 500$ *as a function of the probability of seeking hospitalization* π*. The size of ETUs and burial teams are fixed to* $H_{max} = 1020$ *and* $\mathcal{T} = 20$ *respectively. Change in the parameter* π *seems to affect the epidemic significantly. We can see nearly* 28.80 % *decrease of the total Ebola cases. The parameter values used for this model are in Table 1 updated by Table 3, with* $\mu = 0.85$*.*

We were also interested in knowing how would increased desire for hospitalization along with increased hospital size affect the epidemic. To answer this question we produce a plot of cumulative cases as a function of number of hospital beds and the probability of hospitalization π.

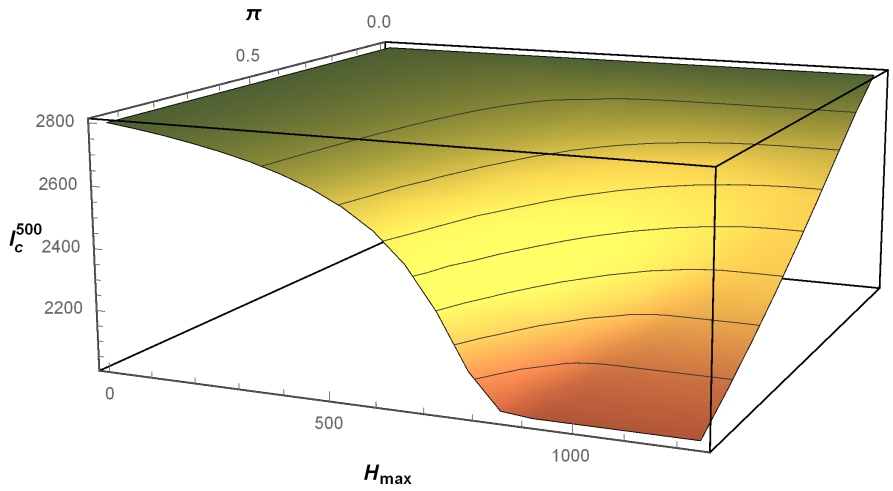

Figure 23: The graph shows the function (4.2) I_c^t *of the model* (M4.4) *at time* $t = 500$ *as a function of the number of hospital beds* H_{max} *and the probability of hospitalization* π*. The number of burial teams is fixed to* $\mathcal{T} = 20$*. The parameter values used for this model are in Table 1 updated by Table 3, with* $\mu = 0.85$*.*

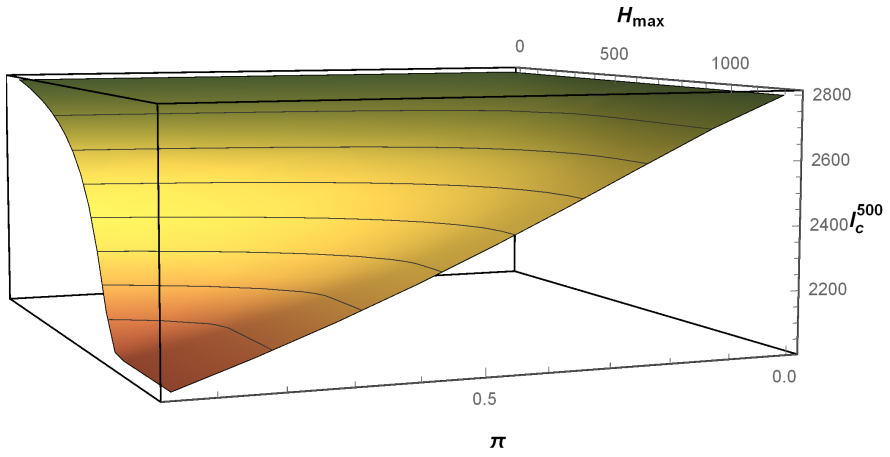

Figure 24: The same as previous Figure but from a different angle.

The last result we would like to present is the comparison of the cumulative cases of the prediction of our model and the real situation for hypothetical choices of the number of hospital beds and burial teams along with the probablity of hospitalization π. We found out in Figure 21 that increasing the number of hospital beds and burial teams only slightly decreases the epidemic size. However, we can observe a significant effect of the probability of seeking hospitalization π in the Figures 25 and 26.

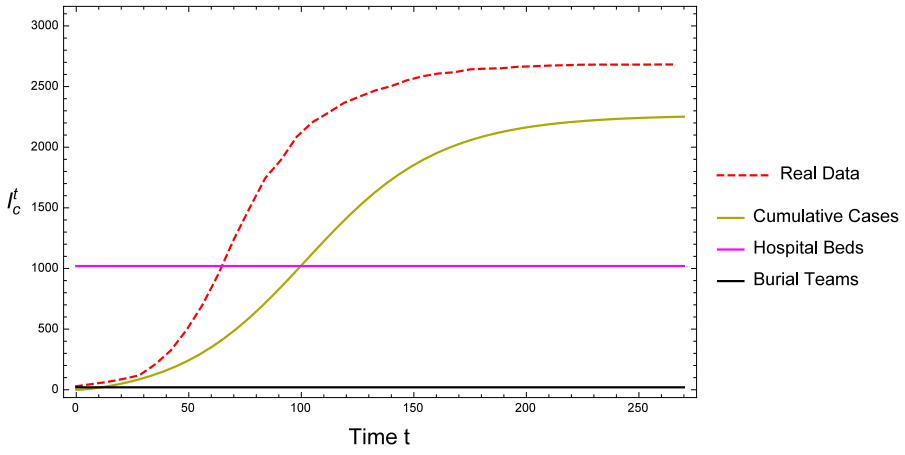

Figure 25: The graph of I_c^t of the model (M4.4)*, with fixed number of burial teams $\mathcal{T} = 20$ and hospital beds $H_{max} = 1020$. The dashed line depicts the real data [8]. The parameter values used for this model are in Table 1 updated by Table 3, with $\mu = 0.85$ and $\pi = 0.5$.*

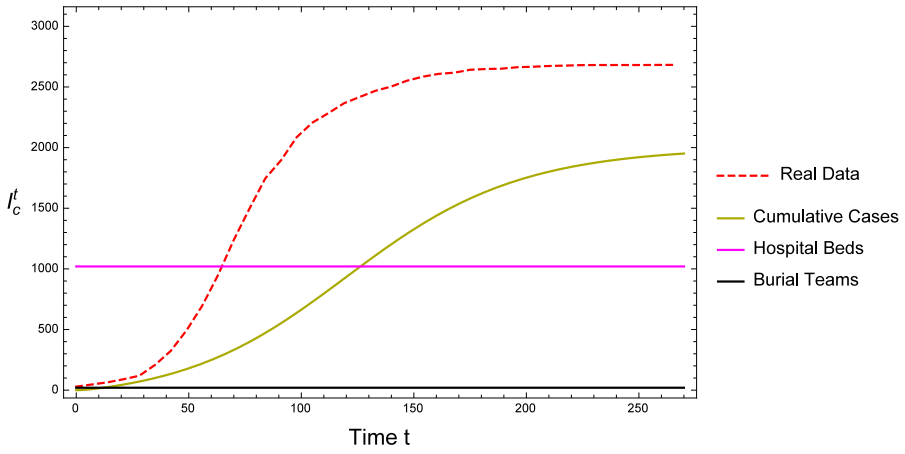

Figure 26: As the previous Figure but with the probability of hospitalization is $\pi = 0.8$. The epidemic is significantly influenced by increasing π.

5 Conclusion

The main goal of this work was to describe effects of strategies for Ebola control. We provided examples of three control approaches: increasing hospital size, introducing burial teams to the population, and increasing the probability of seeking hospitalization. We showed the differences between impacts of these three strategies on the disease dynamic. The population size N and the community contact rates β_{I_R}, β_{I_D} were estimated based on the most recent $2014 - 2015$ Ebola outbreak in west Africa. We found a very close fit of our initial model (M4.1) to the real data. We also discussed the problems of the effective size of the population at risk. It was shown that the effective population at risk is significantly smaller than the actual population size.

We found out that larger hospital size H_{max} would be more influential on the outbreak than the number of burial teams $\mathcal{T}$. It is not surprising that the combined effect of those two would be the best solution for the Ebola control. However, we observed that with fixed number of hospital beds and burial teams, the biggest impact on the epidemic was the desire of population for hospitalization π. This along with increase in hospital size would result in a significant decrease of Ebola casualties.

Effect of Interventions		
Control Strategy	Effect	Level of Control
Hospital Size	4.82 %	0-1200 beds, 0 teams
Burial Teams	1.90 %	0-40 teams, 0 beds
Burial Teams with limited hospital size$^{\heartsuit}$	1.71 %	0-40 teams, 500 beds
Hospital Size & Burial Teams	6.60 %	0-1200 beds, 0-40 teams
Probability of Hospitalization$^{\diamondsuit}$	28.80 %	0-100 %

Table 4: The list of different effects on the epidemic size for the described control strategies. The effects are measured as a difference between certain levels of each intervention. $\heartsuit$: We can observe an interesting result for this case. Limited hospital size causes more total cases overall, which results in burials teams getting busy too fast and not being able to compensate for the surplus of bodies. Therefore, we observe only very small effect of burial teams. $\diamondsuit$: Note that the hospital size and the number of burial teams are $H_{max} = 1020$ and $\mathcal{T} = 20$ respectively.

A possible question for future research is to examine the way of modeling the limited ETU size, which in our model (M4.4) seems to be rather complicated. Our model assumes that everyone who is rejected from the ETU stays in the infectious class and recover/die on their. However, they are allowed to try reentering the hospital. This however, is not clear. Individuals repelled from the hospital may not want to go back or may be incapacitated. For curiosity we tried to model this situation as well. The diagram and the system of differential equations can be found in the Appendix A. The comparison of our model and this new approach is depicted in the following plot.

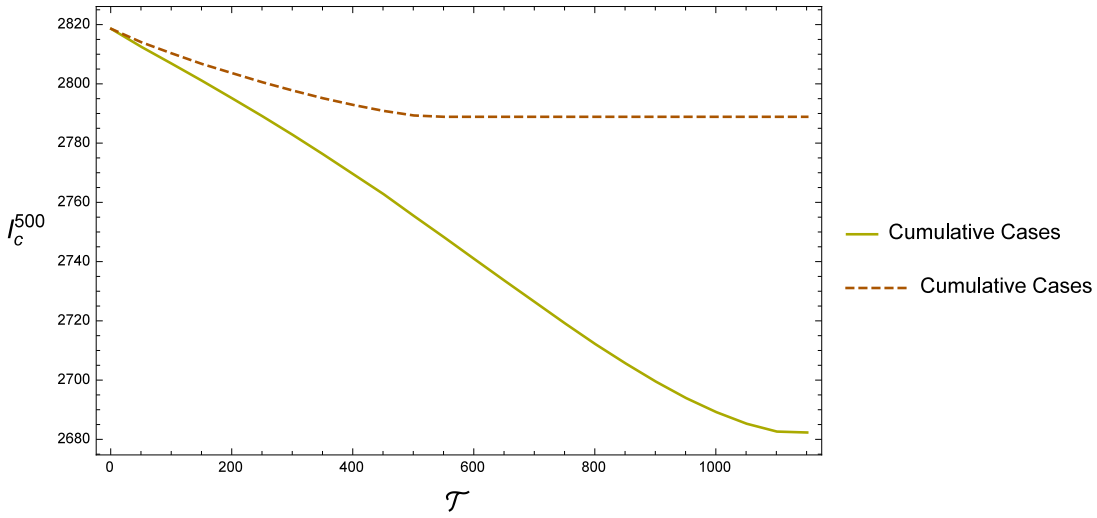

Figure 27: The graph shows the function I_c^t of the models (M4.4) *and* (M4.5) *at time $t = 500$ as a function of the number of hospital beds H_{max}. The solid line represents the prediction from the model* (M4.2) *meanwhile the dashed line depicts the new approach given by* (M4.5). *The new approach yields larger numbers of people exposed to Ebola, explained by people not trying to reenter the hospitals after rejection. The parameter values used for this simulation are in Table 1 updated by Table 3, with $\mu = 0.85$ and $\pi = 0.197$.*

We can observe a significant difference between the two approaches. It would interesting to study a comparison of modeling limited hospitalization and maybe find a way to model a weighted average, meaning that some people when rejected from hospital are willing to come back and try to reenter the hospital meanwhile others are not ever returning.

Another possibility for future work is to describe the parameters μ, π or number of ETU beds and burial teams in a more detailed way. One suggestion is to treat parameters as time dependent. Although we experimented with this approach, the results we obtained were nearly the same or the numerical simulations became problematic.

Therefore, we decided not to pursue this issue at all. A second suggestion is to treat these parameters as independent variables along with time.

Lastly, we could assign a cost to each kind of presented interventions. Then, we would minimize the cost function as an optimization problem to determine cost-effectiveness of the Ebola control strategies described in this paper.

The codes for all the computations and simulations are part of the Appendix B.

6 Appendix A

The system of differential equations for the different approach of modeling limited hospitalization when people rejected from ETUs never try coming back.

$$
\begin{aligned}
\frac{\mathrm{d}S}{\mathrm{d}t} &= -\frac{1}{N}\left[\beta_{I_R} S I_R + \beta_{I_D} S I_D + \beta_{H_R} S H_R + \beta_{H_D} S H_D + \beta_F S F\right], \\
\frac{\mathrm{d}E}{\mathrm{d}t} &= \frac{1}{N}\left[\beta_{I_R} S I_R + \beta_{I_D} S I_D + \beta_{H_R} S H_R + \beta_{H_D} S H_D + \beta_F S F\right] - \alpha E, \\
\frac{\mathrm{d}P_R}{\mathrm{d}t} &= (1-\theta)\alpha E - \epsilon_2 P_R, \\
\frac{\mathrm{d}P_D}{\mathrm{d}t} &= \theta\alpha E - \kappa_2 P_D, \\
\frac{\mathrm{d}I_R}{\mathrm{d}t} &= (1-\pi)\epsilon_2 P_R + \mathrm{If}\left[(H_R + H_D) < \mu H_{max}, 0, \mathrm{Max}\left[0, \pi\epsilon_2 P_R - \Pi\epsilon_2 P_R\right]\right] - \frac{1}{\frac{1}{\epsilon_1} - \frac{1}{\epsilon_2}} I_R, \\
\frac{\mathrm{d}I_D}{\mathrm{d}t} &= (1-\pi)\kappa_1 P_D + \mathrm{If}\left[(H_R + H_D) < \mu H_{max}, 0, \mathrm{Max}\left[0, \pi\kappa_2 P_D - \Pi\kappa_2 P_D\right]\right] - \frac{1}{\frac{1}{\kappa_1} - \frac{1}{\kappa_2}} I_D, \\
\frac{\mathrm{d}H_R}{\mathrm{d}t} &= \mathrm{If}\left[(H_R + H_D) < \mu H_{max}, \pi\epsilon_2 P_R, \mathrm{Min}\left[\pi\epsilon_2 P_R, \Pi\epsilon_2 P_R\right]\right] - \rho H_R, \\
\frac{\mathrm{d}H_D}{\mathrm{d}t} &= \mathrm{If}\left[(H_R + H_D) < \mu H_{max}, \pi\kappa_2 P_D, \mathrm{Min}\left[\pi\kappa_2 P_D, \Pi\kappa_2 P_D\right]\right] - \delta H_D, \\
\frac{\mathrm{d}R}{\mathrm{d}t} &= \frac{1}{\frac{1}{\epsilon_1} - \frac{1}{\epsilon_2}} I_R + \rho H_R, \\
\frac{\mathrm{d}F}{\mathrm{d}t} &= \frac{1}{\frac{1}{\kappa_1} - \frac{1}{\kappa_2}} I_D - \gamma F, \\
\frac{\mathrm{d}D}{\mathrm{d}t} &= \gamma F + \delta H_D.
\end{aligned}
\tag{M4.5}
$$

Note that $\Pi = \dfrac{\rho H_R + \delta H_D}{\epsilon_2 P_R + \kappa_2 P_D}$, derived in the same way as (4.3).

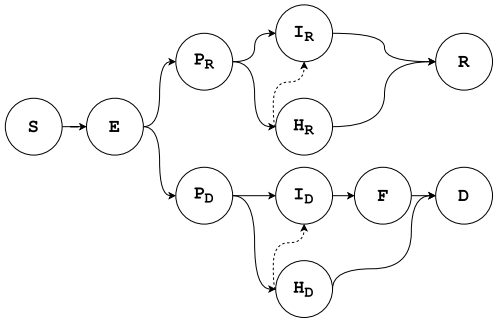

Figure 28: Flow chart of the model (M4.5) *with alternative way of hospitalization.*

7 Appendix B

Mathematica and MATLAB codes used for the numerical simulations and computations.

- MATLAB code for the Reproduction number $\mathcal{R}_0$

```
% Computation of the Reproduction number R0 for the model M1
% Author: Vaclav Hasenohrl

clear all

% parameters
syms beta1 beta2 beta3 beta4 beta5
syms alpha theta epsilon1 kappa1 epsilon2 kappa2 pi delta gamma rho

disp('test');

% matrices F and V defined in the Section 3
F = [0,beta1,beta2,beta3,beta4,beta5;
    0,0,0,0,0,0;
    0,0,0,0,0,0;
    0,0,0,0,0,0;
    0,0,0,0,0,0;
    0,0,0,0,0,0];

V = [alpha,0,0,0,0,0;
    -(1-theta)*alpha,(1-pi)*epsilon1+pi*epsilon2,0,0,0,0;
    -theta*alpha,0,(1-pi)*kappa1+pi*kappa2,0,0,0;
    0,-pi*epsilon2,0,rho,0,0;
    0,0,-pi*kappa2,0,delta,0;
    0,0,-(1-pi)*kappa1,0,0,gamma];

pretty(eig(F*inv(V))) % prints the eigenvalues of FV^-1
```

MATHEMATICA code for the simulation of the Model M4.1 - simulation

```
In[1]:= Manipulate[
        soln = NDSolve[{
          S'[t] == -1/n*(b1*S[t]*Ir[t] + b2*S[t]*Id[t] + b3*S[t]*Hr[t] + b4*S[t]*Hd[t] + b5*S[t]*F[t]),
          Ex'[t] == 1/n*(b1*S[t]*Ir[t] + b2*S[t]*Id[t] + b3*S[t]*Hr[t] + b4*S[t]*Hd[t] + b5*S[t]*F[t]) -
                    a*Ex[t],
          Ir'[t] == (1 - th)*a*Ex[t] - (1 - p)*e1*Ir[t] - p*e2*Ir[t],
          Id'[t] == th*a*Ex[t] - (1 - p)*k1*Id[t] - p*k2*Id[t],
          Hr'[t] == p*e2*Ir[t] - r*Hr[t],
          Hd'[t] == p*k2*Id[t] - d*Hd[t],
          R'[t] == (1 - p)*e1*Ir[t] + r*Hr[t],
          F'[t] == (1 - p)*k1*Id[t] - g*F[t],
          Dh'[t] == g*F[t] + d*Hd[t],
          Cml'[t] == a*Ex[t],
          S[0] == n - Ex0, Ex[0] == Ex0, Ir[0] == 0, Id[0] == 0, Hr[0] == 0,
           Hd[0] == 0, R[0] == 0, F[0] == 0, Dh[0] == 0,
          Cml[0] == 0}, {S[t], Ex[t], Ir[t], Id[t], Hr[t], Hd[t], R[t],
          F[t], Dh[t], Cml[t]}, {t, 0, tmax}];

        Show[Plot[{S[t] /. soln,
          Ex[t] /. soln, (Ir[t] + Id[t]) /. soln, (Hr[t] + Hd[t]) /. soln,
          R[t] /. soln, F[t] /. soln, Dh[t] /. soln}, {t, 0, tmax},
         PlotStyle -> {Blue, Darker[Yellow], Red, Orange, Darker[Green],
           Purple, Black},
         PlotLegends -> {"Susceptibles", "Exposed", "Infectious",
           "Hospitalized", "Recovered", "Funeral", "Deceased"},
         PlotRange -> {{0, tmax}, {0, ymax}}], Frame -> True,
        FrameLabel -> {Style["Time t", Black, Larger],
          Style["N", Black, Larger]}, RotateLabel -> False,
        ImageSize -> 500],

        {{n, 1500000}, 1, 1500000, 1}, {{hmax, 501}, 1, 1200, 1}, {{NT, 25},
        0, 40, 1}, {{p, 0.197}, 0, 1, 0.05}, Delimiter, {{tmax, 700}, 0.01,
        1000, 0.5}, {{ymax, 1500000}, 0, 1500000, 1},
        Initialization :> {n = 1500000, b1 = 0.16, b2 = 0.16, b3 = 0.062,
         b4 = 0.062, b5 = 0.489, a = 1/12, e1 = 1/15, e2 = 1/3.24,
         k1 = 1/13.31, k2 = 1/3.24, th = 0.45049, r = 1/15.88, d = 1/10.07,
         g = 1/2.01, Ex0 = 32, tmax = 700}, ControlPlacement -> Right]
```

MATHEMATICA code for the simulation of the Model M4.1 - fitting of the parameters

```
In[2]:= Manipulate[
soln = NDSolve[{
  S'[t] == -1/n*(b1*S[t]*Ir[t] + b2*S[t]*Id[t] + b3*S[t]*Hr[t] + b4*S[t]*Hd[t] + b5*S[t]*F[t]),
  Ex'[t] == 1/n*(b1*S[t]*Ir[t] + b2*S[t]*Id[t] + b3*S[t]*Hr[t] + b4*S[t]*Hd[t] + b5*S[t]*F[t]) -
            a*Ex[t],
  Ir'[t] == (1 - th)*a*Ex[t] - (1 - p)*e1*Ir[t] - p*e2*Ir[t],
  Id'[t] == th*a*Ex[t] - (1 - p)*k1*Id[t] - p*k2*Id[t],
  Hr'[t] == p*e2*Ir[t] - r*Hr[t],
  Hd'[t] == p*k2*Id[t] - d*Hd[t],
  R'[t] == (1 - p)*e1*Ir[t] + r*Hr[t],
  F'[t] == (1 - p)*k1*Id[t] - g*F[t],
  Dh'[t] == g*F[t] + d*Hd[t],
  Cml'[t] == a*Ex[t],
  S[0] == n - Ex0, Ex[0] == Ex0, Ir[0] == 0, Id[0] == 0, Hr[0] == 0,
   Hd[0] == 0, R[0] == 0, F[0] == 0, Dh[0] == 0,
  Cml[0] == 0}, {S[t], Ex[t], Ir[t], Id[t], Hr[t], Hd[t], R[t],
  F[t], Dh[t], Cml[t]}, {t, 0, tmax}];
Show[{data,
 Plot[{Cml[t] /. soln}, {t, 0, tmax}, PlotStyle -> {Darker[Yellow]},
  PlotLegends -> {"Cumulative Cases"}]}, Frame -> True,
FrameLabel -> {Style["Time t", Black, FontSize -> 16],
  Style["\!\(\*SubsuperscriptBox[\(E\), \(c\), \(t\)]\)", Black,
   FontSize -> 16]}, RotateLabel -> False,
PlotRange -> {{0, tmax}, {0, ymax}}, ImageSize -> 500],

{{n, 2860}, 1, 3500, 1}, {{b1, 0.27}, 0.16, 0.3, 0.005}, {{b2, 0.27},
 0.16, 0.3, 0.005}, {{hmax, 501}, 1, 1200, 1}, {{NT, 25}, 0, 40,
1}, {{p, 0.197}, 0, 1, 0.05}, Delimiter, {{tmax, 700}, 0.01, 1000,
0.5}, {{ymax, 3000}, 0, 1500000, 1},
Initialization :> {n = 2860, b1 = 0.27, b2 = 0.27, b3 = 0.062,
 b4 = 0.062, b5 = 0.489, a = 1/12, e1 = 1/15, e2 = 1/3.24,
 k1 = 1/13.31, k2 = 1/3.24, th = 0.45049, r = 1/15.88, d = 1/10.07,
 g = 1/2.01, Ex0 = 32,
 tmax = 270, {data =
    ListPlot[{{0, 29}, {7, 47}, {14, 65}, {21, 90}, {28, 119}, {35, 208}, {42, 324}, {49, 493},
    {56, 697}, {63, 949}, {70, 1239}, {77, 1498}, {84, 1746}, {91, 1896}, {98, 2087}, {105,
           2207},
    {112, 2284}, {119, 2366},{126, 2418}, {133, 2469}, {140, 2504}, {147, 2552}, {154, 2585},
    {161, 2608}, {168, 2618}, {175, 2642}, {182, 2648}, {189, 2651}, {196, 2663}, {203, 2667},
    {210, 2673}, {217, 2676}, {224, 2680}, {231, 2681}, {238, 2681}, {245, 2681}, {252, 2681},
    {259, 2682}, {266, 2682}},
     Joined -> True, PlotStyle -> {Red, Dashed},
     PlotLegends -> {"Real Data"}];}}, ControlPlacement -> Right]
```

MATHEMATICA code for the simulation of the Model M4.2 - Limited hospital size, I_c^t as a function of H_{max}

In[3]:=
```
n = 2860; b1 = 0.27; b2 = 0.27; b3 = 0.062; b4 = 0.062; b5 = 0.489; a = 1/12;
e1 = 1/15; e2 = 1/3.24; k1 = 1/13.31; k2 = 1/3.24; th = 0.45049; r = 1/15.88;
d = 1/10.07; g = 1/2.01; p = 0.197; mu = 0.85; Ex0 = 32; tmax = 500;


Fn[hmax_] :=
Cml[tmax] /. NDSolve[{
  S'[t] == -1/n*(b1*S[t]*Ir[t] + b2*S[t]*Id[t] + b3*S[t]*Hr[t] + b4*S[t]*Hd[t] + b5*S[t]*F[t]),
  Ex'[t] == 1/n*(b1*S[t]*Ir[t] + b2*S[t]*Id[t] + b3*S[t]*Hr[t] + b4*S[t]*Hd[t] + b5*S[t]*F[t]) - a*Ex[t],
  Ir'[t] == (1 - th)*a*Ex[t] - If[(Hr[t] + Hd[t]) < mu*hmax/4, (1 - p)*e1*Ir[t] + p*e2*Ir[t],
     Max[(1 - ((r*Hr[t] + d*Hd[t])/(e2*Ir[t] + k2*Id[t])))*(e1*Ir[t]), (1 - p)*e1*Ir[t]] +
     Min[(e2*Ir[t])/(e2*Ir[t] + k2*Id[t])*(r*Hr[t] + d*Hd[t]), p*e2*Ir[t]]],
  Id'[t] == th*a*Ex[t] -
    If[(Hr[t] + Hd[t]) < mu*hmax/4, (1 - p)*k1*Id[t] + p*k2*Id[t],
     Max[(1 - ((r*Hr[t] + d*Hd[t])/(e2*Ir[t] + k2*Id[t])))*(k1*Id[t]), (1 - p)*k1*Id[t]] +
     Min[(k2*Id[t])/(e2*Ir[t] + k2*Id[t])*(r*Hr[t] + d*Hd[t]), p*k2*Id[t]]],
  Hr'[t] == If[(Hr[t] + Hd[t]) < mu*hmax/4, p*e2*Ir[t],
  Min[(e2*Ir[t])/(e2*Ir[t] + k2*Id[t])*(r*Hr[t] + d*Hd[t]), p*e2*Ir[t]]]
  - r*Hr[t],
  Hd'[t] == If[(Hr[t] + Hd[t]) < mu*hmax/4, p*k2*Id[t],
     Min[(k2*Id[t])/(e2*Ir[t] + k2*Id[t])*(r*Hr[t] + d*Hd[t]), p*k2*Id[t]]]
     - d*Hd[t],
  R'[t] == If[(Hr[t] + Hd[t]) < mu*hmax/4, (1 - p)*e1*Ir[t],
     Max[(1 - ((r*Hr[t] + d*Hd[t])/(e2*Ir[t] + k2*Id[t])))*(e1*Ir[t]), (1 - p)*e1*Ir[t]]]
     + r*Hr[t],
  F'[t] == If[(Hr[t] + Hd[t]) < mu*hmax/4, (1 - p)*k1*Id[t],
     Max[(1 - ((r*Hr[t] + d*Hd[t])/(e2*Ir[t] + k2*Id[t])))*(k1*Id[t]), (1 - p)*k1*Id[t]]]
     - g*F[t],
  Dh'[t] == g*F[t] + d*Hd[t],
  Cml'[t] == a*Ex[t],
  S[0] == n - Ex0, Ex[0] == Ex0, Ir[0] == 0, Id[0] == 0, Hr[0] == 0,
   Hd[0] == 0, R[0] == 0, F[0] == 0, Dh[0] == 0, Cml[0] == 0}, {S,
  Ex, Ir, Id, Hr, Hd, R, F, Dh, Cml}, {t, 0, tmax},
 Method -> "Adams", AccuracyGoal -> 4, PrecisionGoal -> 4]
```

In[4]:=
```
dat = Table[{x = Hmax, Fn[Hmax][[1]]}, {Hmax, 1, 1200, 30}];
```

In[5]:=
```
plot = ListPlot[dat, Joined -> True, PlotStyle -> Darker[Yellow],
PlotRange -> All, Frame -> True,
FrameLabel -> {Style["\!\(\*SubscriptBox[\(H\), \(max\)]\)", Black,
   FontSize -> 16],
  Style["\!\(\*SubsuperscriptBox[\(E\), \(c\), \(t\)]\)", Black,
   FontSize -> 16]}, RotateLabel -> False, ImageSize -> 500,
PlotLegends -> {"Cumulative Cases"}]
```

MATHEMATICA code for the simulation of the Model M4.3 - Burial Teams, I_c^t as a function of $\mathcal{T}$

```
In[6]:= n = 2860; b1 = 0.27; b2 = 0.27; b3 = 0.062; b4 = 0.062; b5 = 0.489; a = 1/12;
        e1 = 1/15; e2 = 1/3.24; k1 = 1/13.31;k2 = 1/3.24; th = 0.45049; r = 1/15.88;
        d = 1/10.07; g = 1/2.01; p = 0.197; mu = 0.85; f1 = 1; f2 = 0.5; Ex0 = 32;
        tmax = 500;

        Fn[NT_] :=
        Cml[tmax] /. NDSolve[{
          S'[t] ==  -1/n*(b1*S[t]*Ir[t] + b2*S[t]*Id[t] + b3*S[t]*Hr[t] + b4*S[t]*Hd[t] + b5*S[t]*F[t]),
          Ex'[t] ==  1/n*(b1*S[t]*Ir[t] + b2*S[t]*Id[t] + b3*S[t]*Hr[t] + b4*S[t]*Hd[t] + b5*S[t]*F[t])
                    - a*Ex[t],
          Ir'[t] ==  (1 - th)*a*Ex[t] - (1 - p)*e1*Ir[t] - p*e2*Ir[t],
          Id'[t] ==  th*a*Ex[t] - (1 - p)*k1*Id[t] - p*k2*Id[t],
          Hr'[t] ==  p*e2*Ir[t] - r*Hr[t],
          Hd'[t] ==  p*k2*Id[t] - d*Hd[t],
          R'[t] ==  (1 - p)*e1*Ir[t] + r*Hr[t],
          F'[t] == (1 - p)*k1*Id[t] - g*F[t] - NT*f1*F[t]/(f1/f2 + F[t]),
          Dh'[t] == g*F[t] + NT*f1*F[t]/(f1/f2 + F[t]) + d*Hd[t],
          Cml'[t] == a*Ex[t],
          S[0] == n - Ex0, Ex[0] == Ex0, Ir[0] == 0, Id[0] == 0, Hr[0] == 0,
           Hd[0] == 0, R[0] == 0, F[0] == 0, Dh[0] == 0, Cml[0] == 0}, {S,
          Ex, Ir, Id, Hr, Hd, R, F, Dh, Cml}, {t, 0, tmax},
         Method -> "Adams", AccuracyGoal -> 4, PrecisionGoal -> 4]

In[7]:= dat = Table[{x = T, Fn[T][[1]]}, {T, 0, 40, 1}];

In[8]:= plot = ListPlot[dat, Joined -> True, PlotStyle -> Darker[Yellow],
        PlotRange -> All, Frame -> True,
        FrameLabel -> {Style["\[ScriptCapitalT]", Black, FontSize -> 16],
          Style["\!\(\*SubsuperscriptBox[\(E\), \(c\), \(t\)]\)", Black,
           FontSize -> 16]}, RotateLabel -> False, ImageSize -> 500,
        PlotLegends -> {"Cumulative Cases"}]
```

MATHEMATICA code for the simulation of the Model M4.4 - Both interventions, I_c^t as a function of H_{max} and $\mathcal{T}$

```
In[9]:= n = 2860; b1 = 0.27; b2 = 0.27; b3 = 0.062; b4 = 0.062; b5 = 0.489; a = 1/12;
e1 = 1/15; e2 = 1/3.24; k1 = 1/13.31; k2 = 1/3.24; th = 0.45049; r = 1/15.88;
d = 1/10.07; g = 1/2.01; p = 0.197; hmax = 500; mu = 0.85; f1 = 1; f2 = 0.5;
Ex0 = 32; tmax = 500;
Fn[hmax_, NT_] :=
Cml[tmax] /. NDSolve[{
   S'[t] == -1/n*(b1*S[t]*Ir[t] + b2*S[t]*Id[t] + b3*S[t]*Hr[t] + b4*S[t]*Hd[t] + b5*S[t]*F[t]),
   Ex'[t] == 1/n*(b1*S[t]*Ir[t] + b2*S[t]*Id[t] + b3*S[t]*Hr[t] + b4*S[t]*Hd[t] + b5*S[t]*F[t])
             - a*Ex[t],
   Ir'[t] == (1 - th)*a*Ex[t] - If[(Hr[t] + Hd[t]) < mu*hmax/4, (1 - p)*e1*Ir[t] + p*e2*Ir[t],
      Max[(1 - ((r*Hr[t] + d*Hd[t])/(e2*Ir[t] + k2*Id[t])))*(e1*Ir[t]), (1 - p)*e1*Ir[t]] +
      Min[(e2*Ir[t])/(e2*Ir[t] + k2*Id[t])*(r*Hr[t] + d*Hd[t]), p*e2*Ir[t]]],
   Id'[t] == th*a*Ex[t] - If[(Hr[t] + Hd[t]) < mu*hmax/4, (1 - p)*k1*Id[t] + p*k2*Id[t],
      Max[(1 - ((r*Hr[t] + d*Hd[t])/(e2*Ir[t] + k2*Id[t])))*(k1*Id[t]), (1 - p)*k1*Id[t]] +
      Min[(k2*Id[t])/(e2*Ir[t] + k2*Id[t])*(r*Hr[t] + d*Hd[t]), p*k2*Id[t]]],
   Hr'[t] == If[(Hr[t] + Hd[t]) < mu*hmax/4, p*e2*Ir[t],
      Min[(e2*Ir[t])/(e2*Ir[t] + k2*Id[t])*(r*Hr[t] + d*Hd[t]), p*e2*Ir[t]]] - r*Hr[t],
   Hd'[t] == If[(Hr[t] + Hd[t]) < mu*hmax/4, p*k2*Id[t],
      Min[(k2*Id[t])/(e2*Ir[t] + k2*Id[t])*(r*Hr[t] + d*Hd[t]), p*k2*Id[t]]] - d*Hd[t],
   R'[t] == If[(Hr[t] + Hd[t]) < mu*hmax/4, (1 - p)*e1*Ir[t],
      Max[(1 - ((r*Hr[t] + d*Hd[t])/(e2*Ir[t] + k2*Id[t])))*(e1*Ir[t]), (1 - p)*e1*Ir[t]]]
      + r*Hr[t],
   F'[t] == If[(Hr[t] + Hd[t]) < mu*hmax/4, (1 - p)*k1*Id[t],
      Max[(1 - ((r*Hr[t] + d*Hd[t])/(e2*Ir[t] + k2*Id[t])))*(k1*Id[t]), (1 - p)*k1*Id[t]]]
      - g*F[t] -
     NT*f1*F[t]/(f1/f2 + F[t]),
   Dh'[t] == g*F[t] + NT*f1*F[t]/(f1/f2 + F[t]) + d*Hd[t],
   Cml'[t] == a*Ex[t],
   S[0] == n - Ex0, Ex[0] == Ex0, Ir[0] == 0, Id[0] == 0,
   Hr[0] == 0, Hd[0] == 0, R[0] == 0, F[0] == 0, Dh[0] == 0,
   Cml[0] == 0}, {S, Ex, Ir, Id, Hr, Hd, R, F, Dh, Cml}, {t, 0,
   tmax}, Method -> "BDF", AccuracyGoal -> 5, PrecisionGoal -> 5];
```

```
In[10]:= Z = Table[{Hmax, T, Fn2[Hmax,T][[1]]}, {Hmax, 1,
           1250, 65}, {T, 0, 40, 1}];

In[11]:= dat = ArrayReshape[Z, {Dimensions[Z][[1]]*Dimensions[Z][[2]], 3}];

In[12]:= ListContourPlot[dat, InterpolationOrder -> 5,
         Contours -> {2800, 2760, 2720, 2680, 2640, 2634},
         PlotLegends -> Automatic, Frame -> True,
         FrameLabel -> {Style["\!\(\*SubscriptBox[\(H\), \(max\)]\)", Black,
           Larger, Bold], Style["\[ScriptCapitalT]", Black, Larger, Bold]} ,
         olorFunction -> "SandyTerrain", ImageSize -> 500]

In[13]:= ListPlot3D[dat, MeshFunctions -> {#3 &}, Mesh -> {9},
         InterpolationOrder -> 5, ColorFunction -> "SandyTerrain",
         ImageSize -> 500,
         AxesLabel -> {Style["\!\(\*SubscriptBox[\(H\), \(max\)]\)", Black,
           Larger, Bold], Style["\[ScriptCapitalT]", Black, Larger, Bold],
          Style["\!\(\*SubsuperscriptBox[\(E\), \(c\), \(t\)]\)", Black,
           Larger, Bold]}, BoxStyle -> Bold]
```

References

[1] Centers for Disease Control and Prevention. *About Ebola Virus Disease*, available at http://www.cdc.gov/vhf/ebola/about.html, Web. 13 Mar. 2016.

[2] Centers for Disease Control and Prevention. *2014 Ebola Outbreak in West Africa*, available at http://www.cdc.gov/vhf/ebola/outbreaks/2014-west-africa/index.html, Web. 13 Mar. 2016.

[3] W. O. Kermack and A .G. McKendrick, *A Contribution to the Mathematical Theory of Epidemics* Proceedings of the Royal Society of London. Series A, Volume 115, Issue 772 (Aug. 1, 1927), 700-721.

[4] Brauer, F., & Castillo-ChaÌĄvez, C. (2012). *Mathematical models in population biology and epidemiology*. New York: Springer. ISBN 978-1-4614-1685-2

[5] Marisa C. Eisenberg, Joseph N.S. Eisenberg, Jeremy P. D'Silva, Eden V. Wells, Sarah Cherng, Yu-Han Kao, Rafael Meza, *Modeling surveillance and interventions in the 2014 Ebola epidemic*, available at http://arxiv.org/abs/1501.05555v3

[6] World Health Organization. *Liberia: a country, and its capital, are overwhelmed with Ebola cases*, available at http://www.who.int/csr/disease/ebola/one-year-report/liberia/en/, Web. 13 Mar. 2016.

[7] World Health Organization. *Ebola response roadmap - Situation report*, available at http://www.who.int/csr/disease/ebola/situation-reports/en/, Web. 13 Mar. 2016.

[8] World Health Organization. *Data on new cases per epidemic week for Montserrado County*, available at http://apps.who.int/gho/data/view.ebola-sitrep.ebola-country-LBR-LBR008003-20160420-data?lang=en, Web. 13 Mar. 2016.

[9] P. van den Driessche, James Watmough, *Reproduction numbers and sub-threshold endemic equilibria for compartmental models of disease transmission*, 2001, PII: S0025-5564(02)00108-6

[10] Julien Arion, Fred Brauer, P. van den Driessche, James Watmough, Jianhong Wu, *A Final size relation for epidemic models*, Volume 4, Number 2, April 2007, available at http://www.mbejournal.org/

[11] J. Legrand, R. F. Grais, P. Y. Boelle, A. J. Valleron and A. Flahault (2007). *Understanding the dynamics of Ebola epidemics. Epidemiology and Infection*, 135, pp 610-621. doi:10.1017/S0950268806007217.

[12] World Health Organization. *Ebola virus disease*, available at http://www.who.int/mediacentre/factsheets/fs103/en/, Web. 13 Mar. 2016.

[13] Rivers CM, Lofgren ET, Marathe M, Eubank S, Lewis BL. *Modeling the Impact of Interventions on an Epidemic of Ebola in Sierra Leone and Liberia*. PLOS Currents Outbreaks. 2014 Oct 16 . Edition 1. doi: 10.1371/currents.outbreaks.fd38dd85078565450b0be3fcd78f5ccf. Available at http://currents.plos.org/outbreaks/article/obk-14-0043-modeling-the-impact-of-interventions-on-an-epidemic-of-ebola-in-sierra-leone-and-liberia/

[14] Tolbert G. Nyenswah, MPH, Matthew Westercamp, PhD, Amanda Ashraf Kamali, MD, Jin Qin, PhD, Emily Zielinski-Gutierrez, DrPH, Fred Amegashie, MD, Mosaka Fallah, PhD, Bernadette Gergonne, MD, Roselyn Nugba-Ballah, MPH, Gurudev Singh, John M. Aberle-Grasse, MPH, Fiona Havers, MD, Joel M. Montgomery, PhD, Luke Bawo, MPH, Susan A. Wang, MD, Ronald Rosenberg, ScD. *Evidence for Declining Numbers of Ebola Cases - Montserrado County, Liberia, June - October 2014*. CDC MMWR Weekly Report. Available at http://www.cdc.gov/mmwr/preview/mmwrhtml/mm63e1114a2.htm

[15] Cassidy Hallaway, *A Mathematical Model of the Ebola Epidemic*, University of Minnesota Undergraduate Research Project Final Report, Department of Mathematics and Statistics, Spring, 2015.

[16] Xinsheng Zhang, *Analysis of Ebola Disease Model with Hospitalization*, University of Minnesota UROP Undergraduate Research Project Final Report, Department of Mathematics and Statistics, Spring, 2016.